RAMA: The Research Moored Array for African-Asian-Australian Monsoon Analysis and Prediction

M. J. McPhaden[(1)], G. Meyers[(2)], K. Ando[(3)],Y. Masumoto[(4)], V. S. N. Murty[(5)], M. Ravichandran[(6)], F. Syamsudin[(7)] J. Vialard[(8)], L. Yu[(9)], W. Yu[(10)]

(1) NOAA/Pacific Marine Environmental Laboratory, Seattle, WA, USA (michael.j.mcphaden@noaa.gov), (2) University of Tasmania, Hobart, Australia, (3) Japan Agency for Marine Earth Science and Technology, Yokosuka, Japan, (4) University of Tokyo, Tokyo, Japan, (5) National Institute of Oceanography, Regional Center, Visakhapatnam, India, (6) Indian National Center for Ocean Information Services, Hyderabad, India, (7) Agency for the Assessment and Application of Technology (BPPT), Indonesia, (8) IRD/Laboratoire d'Océanographie et du Climat: Expérimentation et Approches Numériques Paris, France, (9) Woods Hole Oceanographic Institution, Woods Hole, MA, USA, (10) First Institute of Oceanography, Qingdao, China

Bulletin of the American Meteorological Society, in press

29 September 2008

Capsule

A new moored buoy array in the historically data sparse Indian Ocean provides measurements to advance monsoon research and forecasting.

Abstract

The Indian Ocean is unique among the three tropical ocean basins in that it is blocked at 25°N by the Asian land mass. Seasonal heating and cooling of the land sets the stage for dramatic monsoon wind reversals, strong ocean-atmosphere interactions, and intense seasonal rains over the Indian subcontinent, Southeast Asia, East Africa, and Australia. Recurrence of these monsoon rains is critical to agricultural production that supports a third of the world's population. The Indian Ocean also remotely influences the evolution of El Niño and the Southern Oscillation (ENSO), the North Atlantic Oscillation (NAO), North American weather, and Atlantic hurricane activity. Despite its importance in the regional and global climate system though, the Indian Ocean is the most poorly observed and least well understood of the three tropical oceans.

This article describes the ***R***esearch Moored ***A***rray for African-Asian-Australian ***M***onsoon ***A***nalysis and Prediction (RAMA), a new observational network designed to address outstanding scientific questions related to Indian Ocean variability and the monsoons. RAMA is a multi-nationally supported element of the Indian Ocean Observing System (IndOOS), a combination of complementary satellite and *in situ* measurement platforms for climate research and forecasting. The article describes the scientific rationale, design criteria, and progress towards implementing the array. Initial RAMA data are presented to illustrate how they contribute to improved documentation and understanding of phenomena in the region. Potential future applications of the data for societal benefit are also described.

1. Introduction

The Indian Ocean is unique among the three tropical ocean basins in that it is blocked at 25°N by the Asian land mass. Seasonal heating and cooling of the land sets the stage for dramatic monsoon wind reversals and intense seasonal rains over the Indian subcontinent, Southeast Asia, East Africa, and Australia. The Asian landmass also blocks the ocean to the north so that currents cannot carry heat from the tropics to higher northern latitudes as in the other oceans. Ocean-atmosphere interactions in the region are highly dynamic, involving seasonal current reversals associated with monsoon wind forcing and significant exchanges of heat across the air-sea interface. The Indian Ocean also receives heat from the Pacific via the Indonesian Throughflow (Gordon, 2001) while exporting heat to the Atlantic via the Aguhlas Current system (de Ruijter et al, 1999).

Monsoon rains occur each year, supporting agricultural production that provides food for a third of the world's population. These rains are irregular, however, leading to years of drought or flood that have significant socio-economic consequences (Webster et al, 1998). Failure of Indian summer monsoon rains in 2002 (Waple and Larimore, 2003) and excessive rains in equatorial East Africa in late 2006 (Arguez, 2007) are recent examples of major disasters. Atmospheric teleconnections carry the effects of Indian Ocean climate anomalies to other regions of the globe, where they affect evolution of El Niño and the Southern Oscillation (ENSO) (McPhaden, 1999; Zhang, 2005), the North Atlantic Oscillation (Hoerling et al, 2001), Sahel rainfall (Giannini et al, 2003), Atlantic hurricane formation (Maloney and Hartmann, 2000), the atmospheric circulation of the North Pacific (Annamalai et al, 2007) and western U.S. weather (Higgins and Mo, 1997). Thus, the potential benefits of improved description, understanding and prediction of the

coupled ocean–atmosphere system in the Indian Ocean are enormous. However, the present lack of comprehensive data records for the Indian Ocean severely limits our knowledge of key physical processes and our ability to provide reliable monsoon forecasts even one season ahead.

Observational efforts in the Indian Ocean date back to the International Indian Ocean Expedition of the 1960s (Knauss, 1961; National Research Council, 2000) which was the first comprehensive study of Indian Ocean circulation and water mass properties. In the 1970s, the Indian Ocean Experiment (INDEX; Luyten and Roemmich, 1982) and the Summer Monsoon Experiment (MONEX; Krishnamurti, 1985) were designed to improve the description and understanding of seasonally varying oceanic and atmospheric circulation, respectively. The 10-year (1985-94) Tropical Ocean Global Atmosphere (TOGA) program (National Research Council, 1996) and the World Ocean Circulation Experiment (Siedler et al, 2001) with a field phase from 1990-98 were major international efforts to study ocean-atmosphere interactions and basin scale ocean circulation patterns related to climate. Short term, regional studies such as the Bay of Bengal Monsoon Experiment (Bhat et al, 2000), the Arabian Sea Monsoon Experiment (Sanjeeva Rao and Sikka, 2005) and the Joint Air-Sea Monsoon Experiment (Webster et al, 2002) complemented these broad scale programs by examining key physical processes controlling variability in specific areas of the Indian Ocean. In contrast to those studies which focussed on physical oceanography, ocean-atmosphere interactions, and climate variability, the Joint Global Ocean Flux Study Arabian Sea Expedition (Smith, 2001) of the mid-1990s emphasized ocean biogeochemical cycles and biological productivity in relation monsoon forcing.

These programs laid a foundation for understanding oceanic and atmospheric variability related to the monsoons, but they did not leave a significant legacy of sustained ocean observations in the region (e.g. McPhaden et al, 1998). Development of a tropical Indian Ocean observing system progressed very slowly in part because Indian Ocean sea surface temperature (SST) anomalies on interannual time scales were most often within the range of observational errors (e.g. Annamalai and Murtugudde, 2004), because there was debate about whether ocean dynamics played a major role in their predictability, and because "the predictive relationship between Indian Ocean SST and monsoon rainfall have remained especially poorly characterized…" (Clark et al, 2000). By contrast, during TOGA and continuing through late 1990s as part of the follow-on Climate Variability and Predictability (CLIVAR) program, efforts in tropical ocean observing system development were focussed heavily on the Pacific and Atlantic where ocean-atmosphere interactions were better understood and seasonal prediction efforts were more advanced. The remoteness of the Indian Ocean from first world countries of North America, Europe, and Asia was also a factor in the relatively slow development of an Indian Ocean observing system compared to the Pacific and Atlantic.

The past 10 years have seen a rebirth of interest in the Indian Ocean stimulated by the prominence of the 1997 Indian Ocean Dipole (IOD[1]) event (Saji et al, 1999; Webster et al, 1999; Murtugudde et al, 2000). This event highlighted the dramatic nature and climatic consequences of ocean-atmosphere interactions in the Indian Ocean. The event also drew attention to the relative dearth of measurements in the Indian Ocean and the opportunities to develop a systematic and sustained ocean observing system there.

[1] The Indian Ocean Dipole is also sometimes referred to as the Indian Ocean Dipole Zonal Mode, or IODZM.

94 This paper describes the rationale for and design of a sustained, basin-scale
95 moored buoy array referred to as the ***R***esearch Moored ***A***rray for African-Asian-
96 Australian ***M***onsoon ***A***nalysis and Prediction (RAMA[2]). The array complements other
97 elements of the recently designed Indian Ocean Observing System (IndOOS) which
98 collectively represents an Indian Ocean contribution to the Global Ocean Observing
99 System (GOOS) (CLIVAR-GOOS Indian Ocean Panel, 2006; Meyers and Boscolo,
100 2006). IndOOS in general, and RAMA in particular, address the need to establish a
101 system for comprehensive, long term, high quality, real-time measurements in the Indian
102 Ocean suitable for climate research and forecasting. The broad range of time scales and
103 rapid changes that can occur in the Indian Ocean dictate the need for a moored buoy array
104 providing time series data with high temporal resolution as an essential element of
105 IndOOS. In this respect, RAMA is the Indian Ocean equivalent of the Tropical
106 Atmosphere Ocean/Triangle Trans Ocean Buoy Network (TAO/TRITON; McPhaden et
107 al, 1998; Kuroda and Amitani, 2000) and the Prediction and Research Moored Array in
108 the Tropical Atlantic (PIRATA; Bourles et al, 2008), which respectively anchor basin
109 scale observing systems in the tropical Pacific and Atlantic Oceans. RAMA is targeted at
110 understanding and prediction of the east African, Asian, and Australian monsoons, but it
111 will benefit nations outside the Indian Ocean region because of atmospheric
112 teleconnections that influence the far field. In addition, real-time RAMA data will
113 contribute to improved weather and marine forecasts, like those for tropical cyclones and
114 storm surge. Even though the array is in the initial stages of implementation, the data are
115 already finding practical applications as illustrated in the side bar on Australian farmers.

[2] In Hindu mythology, Rama is an ancient king of India and the hero of the epic "Ramayana".

116 The remainder of this paper is organized as follows. We first briefly review the
117 range of phenomena that motivate the study of climate variability in the Indian Ocean
118 region. Emphasis is on intraseasonal to interannual time scales and the upper ocean north
119 of 30°S where RAMA will have its greatest impact. The reader is referred to Schott et al
120 (2008) for a more complete account of Indian Ocean phenomenology including western
121 boundary currents , the Indonesian Throughflow, major surface currents, and the cross-
122 equatorial overturning circulation. We then describe IndOOS and the design criteria for
123 RAMA, followed by a progress report on RAMA implementation. Examples of RAMA
124 data are presented to illustrate their value for research applications, after which we
125 conclude with a brief summary and discussion.

126 2. Indian Ocean Phenomenology

127 Hallmark attributes of the Indian Ocean climate system are the dramatic reversals
128 of the surface winds propelled by seasonally varying land-ocean temperature contrasts.
129 Equally dramatic are the seasonally varying wind-driven ocean currents that affect the
130 evolution of SST (Fig. 1; see also Schott and McCreary, 2001 and Schott et al, 2008).
131 Associated with monsoon wind variations are pronounced seasonal shifts in atmospheric
132 convection and rainfall over East Africa, southern and eastern Asia, and northern
133 Australia. Collectively, these variations are a regional manifestation of seasonal changes
134 in the Hadley and Walker Circulations, which extend throughout the global tropics.

135 In boreal winter, Northeast Monsoon winds converge with Southeast trade winds
136 in the Intertropical Convergence Zone (ITCZ) located between 5°-12°S. These wind
137 systems drive a surface ocean circulation that features broad, westward flowing currents
138 on either side of the equator—the Northeast Monsoon Current and South Equatorial

Current—and a southward flowing Somali Current along the east coast of Africa. Sandwiched between the two westward currents is the eastward flowing Equatorial Countercurrent, in geostrophic balance with meridional density contrasts in the Seychelles-Chagos thermocline ridge region (Hermes and Reason, 2008; Yokoi et al, 2008). This thermocline ridge, formed by wind stress curl driven upwelling in the ITCZ, rises to within 20 m of the surface and results in a zonal band of very thin mixed layers. SST variations here are sensitive to surface heat fluxes and vertical turbulent heat exchanges with the thermocline because of the low heat capacity of these thin mixed layers (Duvel and Vialard, 2007). Seasonal time scale SST anomalies in this region can moreover remotely influence subsequent development of summer monsoon rainfall along the western Ghats (Vecchi and Harrison, 2004; Izumo et al, 2008).

Wind and circulation patterns in boreal summer are radically different from those in boreal winter. Southwest Monsoon winds drive the currents north of the equator to the east and weaken both the countercurrent and the thermocline ridge. Intense wind-driven coastal upwelling during summer off the Horn of Africa leads to cooling and, through the supply of nutrient rich thermocline water, high biological productivity in the Arabian Sea. This upwelling is fed by a cross equatorial circulation cell that is unique to the Indian Ocean, with source waters formed in the southeastern Indian Ocean (~20°-30°S) flowing northward at thermocline depth to the Arabian Sea (Schott et al, 2004). SSTs in Bay of Bengal on the other hand remain relatively high during summer, stoking the growth of cyclones that often have devastating impacts on surrounding countries. These high SSTs result in part from a strongly salt stratified upper ocean capped by shallow fresh water mixed layers that trap surface heat fluxes and inhibit mixing with the thermocline (Shenoi

et al, 2002). River runoff and open ocean rainfall supply the fresh water to needed to maintain these thin mixed layers.

During the transition seasons between the Northeast and Southwest Monsoons, winds along the equator are westerly. These winds force the eastward flowing "Wyrtki Jets" (Wyrtki, 1973) in April-May and October-November of each year. The Wyrtki Jets are important in transporting mass from west to east along the equator and play an important role in the seasonal heat balance of the basin. They are also dynamically linked to variability off of Sumatra and Java through equatorial and coastal waveguide processes (Wijffels and Meyers, 2004).

Embedded within the seasonally varying monsoons are energetic intraseasonal oscillations (or ISOs) on weekly to monthly time scales. The best known form of ISO is the Madden-Julian Oscillation (MJO), an eastward propagating wave-like phenomenon in the atmosphere with periods of roughly 30-60 days (Madden and Julian, 1994; Zhang, 2005). MJO convection is spawned over the Indian Ocean and subsequently propagates eastward as part of a planetary scale fluctuation in upper tropospheric winds. Variability in surface winds and deep atmospheric convection is most energetic in regions of warm SST ($\geq 27°C$), where interaction with the oceanic mixed layer plays an important role in organizing the MJO (Waliser et al, 1999). Along the equator, intraseasonal wind forcing generates energetic eastward propagating oceanic Kelvin waves (Han, 2005; Fu, 2007) which, upon encountering Sumatra, continue poleward as coastally trapped waves. The majority of coastally trapped intraseasonal wave energy propagating southeastward off Sumatra and Java eventually leaks into the Indonesian Seas through the Lombok Strait where it affects Throughflow transports (Syamsudin et al, 2004).

185 The MJO is strongest in boreal winter and spring in the southern tropics, with a
186 secondary peak during boreal summer north of the equator (Zhang, 2005). During boreal
187 winter, ocean-atmosphere interactions are particularly strong with large intraseasonal
188 SST variations in the vicinity of the shallow Seychelles-Chagos thermocline ridge (Duvel
189 and Vialard, 2007; Vialard et al, 2008a,b). In boreal summer, the MJO spins off cloud
190 and rain bands near the equator that propagate poleward over the Bay of Bengal,
191 contributing to alternating "active" periods of enhanced rainfall and "break" periods of
192 reduced rainfall over the Indian Subcontinent (Madden and Julian, 1994). The number
193 and duration of active/break periods in a particular year determines the net seasonal
194 monsoon rainfall. For this reason intraseasonal oscillations are often referred to as the
195 "building block of the monsoons."
196 There are a variety of significant multi-time scale interactions involving the MJO.
197 For instance, the MJO strongly modulates variability associated with the Wyrtki Jets
198 (Han et al, 2004; Masumoto et al, 2005; Sengupta et al, 2007). The diurnal cycle is
199 important in modulating MJO SST variability and ocean feedbacks to the atmosphere
200 (Woolnough et al, 2007). Synoptic time scale cyclones often develop in association with
201 the MJO (Liebmann et al, 2004; Bessafi and Wheeler, 2006; Seiki and Takayabu, 2007).
202 Positive IOD events tend to suppress the MJO and as well as higher frequency
203 atmosphere fluctuations as a result of the reduced convection over the eastern Indian
204 Ocean (Shinoda and Han, 2005). Farther afield, propagation of the MJO into the western
205 Pacific affects the evolution of ENSO (McPhaden, 1999; McPhaden et al, 2006; Zhang,
206 2005). The MJO likewise influences the development of Atlantic hurricanes (Maloney
207 and Hartmann, 2000) and winter storms along the west coast of the U.S. (Higgins and

208 Mo, 1997). There are other notable intraseasonal variations in the Indian Ocean region
209 besides the MJO, such as an oscillation in sea level with a spectral peak at periods near
210 90 days that Han (2005) attributes to a wind-forced basin scale oceanic resonance.
211 The Indian Ocean is characterized by considerable interannual variability, the
212 most prominent mode of which is the response to remote forcing from ENSO (Yamagata
213 et al, 2004; Schott et al, 2008). An eastward shift in the ascending branch of Walker
214 circulation into the central Pacific during El Niño leads to anomalous subsidence,
215 suppressed convection, high atmospheric surface pressure, and anomalous easterlies over
216 the Indian Ocean. El Niño's impact on precipitation includes reduced Indian summer
217 monsoon rainfall, reduced rainfall in South Africa and Indonesia, and enhanced rainfall in
218 equatorial east Africa. In boreal spring following the peak of El Niño, basin scale
219 warming occurs due to a combination of increased surface heat fluxes and, south of the
220 equator, downwelling Rossby waves forced by anomalous ENSO-induced surface wind
221 stresses (Xie et al, 2002; Yu et al, 2005; Schott et al, 2008). The amplitude of this
222 warming is relatively small compared to that in the tropical Pacific, but it leads to
223 increased tropical cyclone activity in the southwest (Xie et al, 2002) and increased
224 rainfall during the following summer over much of the basin (Yang et al, 2007). .
225 Oceanic and atmospheric anomalies of opposite sign are evident in the Indian Ocean
226 region associated with La Niña events.
227 Another prominent mode of interannual variability in the Indian Ocean is the
228 IOD. Positive IOD events are characterized by anomalously cold SSTs and suppressed
229 atmospheric convection off Java and Sumatra, warm SSTs and enhanced convection off
230 east Africa, easterly wind anomalies along the equator, and a weak boreal fall season

231 Wyrtki Jet (Fig. 2). The IOD is a mode of coupled ocean-atmosphere variability that, like
232 ENSO, develops via feedbacks between zonal wind stress, SST and thermocline depth
233 anomalies. Unlike ENSO, it is shorter lived and confined mostly to the boreal fall
234 season. Annual mean winds along the equator are westerly in Indian Ocean, tilting the
235 thermocline down to the east. Thus, it is only during the normal September to November
236 upwelling season off the coast of Java and Sumatra when the thermocline is brought close
237 enough to the surface that ocean-atmosphere feedbacks can take hold. After that, the
238 strong seasonality associated with the onset of the Northeast Monsoon overwhelms any
239 SST anomalies in this upwelling region that may have developed during the previous
240 summer and fall.

241 The most recent positive IOD events of significant amplitude occurred in 1994,
242 1997, and 2006 (Fig. 2e). These events typically lead to above normal rainfall in East
243 Africa, India, and Southeast Asia and dry conditions in Indonesia and Australia
244 (Yamagata et al, 2004). Far field impacts of the IOD have also been reported on the
245 seasonal climate of East Asia, Brazil, and Europe (*op. cit.*). Negative IOD events develop
246 with anomalies and climatic impacts roughly opposite to those of positive events.

247 There is a tendency for positive IOD events to co-occur with El Niño and negative
248 events with La Niña (Meyers et al, 2007). These co-occurrences have complicated the
249 identification of IOD vis-à-vis ENSO climate impacts and have raised the question of
250 whether the IOD is fundamentally tied to ENSO (e.g., Chang et al, 2006). However, co-
251 occurrences with ENSO do not account for all IOD events and the dynamical ocean
252 response to ENSO vs. purely IOD wind forcing is not identical (Yu et al, 2005). Thus,
253 while ENSO may be an important triggering mechanism, the IOD appears to exist as an

254 independent mode of climate variability (Schott et al, 2008).

255 In addition to interannual variability, the Indian Ocean also experiences longer
256 term decadal variations and trends. For example, there is a decadal modulation in the
257 frequency of IOD events (Ashok et al, 2004), in the relationship between ENSO and the
258 IOD (Schott et al, 2008), and in the relationship between ENSO and Indian summer
259 monsoon rainfall (Krishna-Kumar et al, 1999). Decadal changes in Indian Ocean
260 circulation have been documented, including a decrease in strength of the Indonesian
261 Throughflow since 1976 (Wainwright et al., 2008) and an intensification around 2000 of
262 the subtropical cell (Lee and McPhaden, 2008), which links upwelling in the Seychelles-
263 Chagos thermocline ridge to source waters formed between 20°-30°S in the southeastern
264 basin. Superimposed on these decadal variations are significant multi-decadal warming
265 trends in SST (Cane et al, 1997) and increases in upper ocean heat content (Levitus et al,
266 2005) that may plausibly be attributed to anthropogenic greenhouse gas forcing. The SST
267 trend has been linked to drought in the African Sahel (Giannini et al., 2003) and in the
268 northern hemisphere mid-latitudes (Hoerling and Kumar, 2003). Latent heat fluxes have
269 increased steadily since the early 1980s over the Indian Ocean (Yu and Weller, 2007)
270 suggesting that changes in surface fluxes are a response to, rather than the cause of, this
271 SST trend. It is likely therefore that ocean dynamics play a role in producing the observed
272 SST trend, although the precise mechanisms remain uncertain (Alory et al, 2007).

273 In summary, there is a broad spectrum of phenomena in the Indian Ocean, ranging
274 from diurnal to decadal time scales, that contributes to the observed variability.
275 Quantitative understanding of these phenomena, and how they interact with one another,
276 is undermined though by a sparseness of data. Unlike in the Pacific Ocean where

systematic observations as part of the ENSO observing system were initiated in the early 1980s, there are no high quality multi-decade in situ data records in the upper Indian Ocean except for those from a few ship-of-opportunity expendable bathythermograph (XBT) lines (Feng et al, 2001; Feng and Meyers, 2003). These limitations make it difficult to assess with confidence whether the Indian Ocean-atmosphere system is changing, or may change, as a result of greenhouse gas forcing (Harrison and Carson, 2007).

Data limitations also constrain our ability to develop, initialize, and validate coupled ocean-atmosphere forecast models for monsoon prediction. Experimental forecasting with these models is in its infancy, and there are preliminary indications that skillful seasonal forecasts in the Indian Ocean region may be possible at 2-3 season lead times based on ENSO and IOD influences (Luo et al, 2007; Cherchi et al, 2007). Present levels of skill are limited by poor initialization of the subsurface ocean (Wajsowicz, 2005), systematic errors in ocean and atmospheric models, and the general inability of either atmospheric general circulation models or coupled ocean-atmosphere models to accurately simulate intraseasonal variability like the MJO (Slingo et al, 1996; Zhang, 2005). There is evidence to suggest that elements of this intraseasonal variability may be predictable up to 30 days in advance (Webster and Hoyos, 2004; Miura et al, 2007), so the fact that this variability is not well represented in dynamical prediction models represents a major challenge in both climate and weather forecasting.

3. RAMA as a contribution to IndOOS

3.1 IndOOS

299 The International GOOS program and the Climate Variability and Predictability
300 (CLIVAR) component of the World Climate Research Program (WRCP) established an
301 Indian Ocean Panel (IOP) in 2004 to design, and guide the implementation of, a basin-
302 scale, integrated Indian Ocean observing system for climate research and forecasting. The
303 IOP focused on developing a strategy for *in situ* measurements to complement existing
304 and planned satellite missions for surface winds, sea level, SST, rainfall, salinity, and
305 ocean color. The resulting system, referred to as IndOOS (Fig. 3), is based on proven
306 technologies, including moorings, Argo floats, ship-of-opportunity measurements,
307 surface drifters, and tide gauge stations (CLIVAR-GOOS Indian Ocean Panel, 2006;
308 Meyers and Boscolo, 2006). Transmission of data to shore in real-time via satellite relay,
309 where feasible, was given high priority to promote use of the data in climate analysis and
310 forecast products. Network design emphasized the measurement of physical climate
311 variables but recognized that as the science matures and technology advances,
312 widespread inclusion of biogeochemical measurements to support studies of the ocean
313 carbon cycle and ecosystem dynamics would also be possible.

314 Embedded in this basin scale observing system are regionally focused national
315 observing systems. These include Indian efforts in the Bay of Bengal and Arabian Sea,
316 the Australian Integrated Marine Observing System (IMOS; Meyers and Proctor, 2008)
317 and the Longterm Ocean Climate Observations (LOCO; Ridderinkhof and De Ruijter,
318 2003) for western boundary currents in the Mozambique Channel. In addition, IndOOS
319 provides a long-term, broad scale spatial and temporal context for short duration,
320 geographically focused process studies, such as the Mirai Indian Ocean cruise for the
321 Study of the MJO convection Onset (MISMO; Yoneyama et al, 2008) , the Validation of

322 the Aeroclipper System under Convective Occurrences (VASCO)-Cirene program
323 (Duvel et al, 2008; Vialard et al, 2008a), and International Nusantara Stratification and
324 Transport (INSTANT) program to study the Indonesian Throughflow (Gordon, 2005).
325 3.2 RAMA
326 A key element of IndOOS is the basin-scale moored buoy array, which we call
327 RAMA (Fig. 4). Some of the Indian Ocean programs described in the Introduction
328 collected 1-3 year long time series records either near the equator (Knox, 1976; Reppin et
329 al, 1997) or in the Arabian Sea (Rudnick et al, 1997). Despite these noteworthy efforts
330 though, there has been no plan until now for a coordinated, multi-national, basin-scale
331 sustained mooring array like TAO/TRITON in the Pacific and PIRATA in the Atlantic.
332 RAMA addresses the need for such an array. It is designed specifically for
333 studying large-scale ocean-atmosphere interactions, mixed-layer dynamics, and ocean
334 circulation related to the monsoons on intraseasonal to decadal time scales. The planned
335 array consists mainly of 38 surface moorings eight subsurface moorings (see box). Five
336 of the eight subsurface moorings are Acoustic Doppler Current Profiler (ADCP)
337 moorings to provide long time series measurements of currents in the upper 300-400 m.
338 Four of these ADCP moorings are located along the equator where geostrophy breaks
339 down and direct current measurements are necessary. A fifth ADCP mooring is also
340 located in the upwelling zone off the coast of Java where the SST anomalies associated
341 with the IOD first develop. This mooring is near the northern terminus of the frequently
342 repeated Australia-to-Indonesia XBT line (Fig. 3) providing upper ocean temperature
343 observations at weekly intervals. The primary focus of the array is the upper 500 m,
344 where the ocean and atmosphere most immediately communicate with one another and

345 where intraseasonal-to-decadal time scale variability is most pronounced. However, in
346 addition to the 38 surface and five ADCP moorings, three subsurface moorings along the
347 equator at 77°E, 83°E, and 93°E are designed to monitor ocean currents down to 4000 m
348 (Murty et al, 2006).

349 The array is intended to cover the major centers of ocean–atmosphere interaction
350 in the open ocean away from western boundary current regions and the Indonesian
351 marginal seas. These regions include the Arabian Sea and the Bay of Bengal; the
352 equatorial waveguide where wind-forced intraseasonal and semi-annual current variations
353 are prominent; the eastern and western poles of the IOD; the thermocline ridge between
354 5-12°S, where wind-induced upwelling and Rossby waves affect SST; the southwestern
355 tropical Indian Ocean, where ocean dynamics and air–sea interaction affect cyclone
356 formation (Xie et al., 2002); and the southeastern basin where source waters of the cross
357 equatorial and subtropical circulation cells are formed (Schott et al, 2004). Numerical
358 model design studies have assessed the adequacy of the array to achieve its purposes in
359 the context of other observing system components. Alternative sampling strategies have
360 also been evaluated with the conclusion that the proposed array configuration is
361 scientifically sound and cost-effective (Vecchi and Harrison, 2007; Oke and Schiller,
362 2007).

363 Surface heat and moisture fluxes are important in determining mixed layer
364 temperature and salinity variability. However, surface heat and moisture flux
365 climatologies are poorly known in the Indian Ocean (Yu and McCreary, 2004;
366 Yaremchuk, 2006; Yu et al, 2007) and in several regions annual means in net surface heat
367 flux from presently available climatologies typically differ by 30-40 W m^{-2} (Fig. 5).

Hence, in each of the key regions described above, plans call for at least one specially instrumented surface mooring as a surface flux reference site.

Surface mooring data are telemetered to shore in real-time from the via the Service Argos satellite relay system. Service Argos then places these data on the Global Telecommunications System (GTS) for transmission to operational weather, climate, and ocean forecasting centers. Internally recorded data from all moorings are post-processed and quality controlled on recovery, after which they are then posted on World Wide Web for public distribution (see box on RAMA Moorings). The RAMA data policy is based on the principle of free, open, and timely access to all data from the array.

4. Progress Towards Implementation of RAMA

At the end of 2008, RAMA was 47% complete, with 22 of the 46 mooring sites occupied (Fig. 4). Nations that have provided mooring equipment, ship time, personnel, and/or logistic support so far include Japan, India, the United States, Indonesia, China, France and eight African countries that comprise the Agulhas and Somali Current Large Marine Ecosystems (ASCLME) Project. Contributing organizations and their year of initial involvement are described in the Implementation Time Line side box. Given current and projected national resource commitments, the array could be fully implemented by the end of 2012. The CLIVAR-GOOS Indian Ocean Panel and the CLIVAR Tropical Moored Buoy Implementation Panel provide scientific and technical guidance, respectively, for the development of RAMA.

The array will require a reliable, regular supply of ship time to fully implement since the surface moorings have a design lifetime of one year and must be replaced annually. Making reasonable assumptions about ship speeds, carrying capacity, and ports

391 of call around the Indian Ocean, We estimate that a minimum of approximately 150 days
392 of dedicated ship time per year will be required to maintain the array once complete. For
393 perspective, this requirement is about half that needed to maintain the 70 mooring
394 TAO/TRITON array in the Pacific and about twice that needed to maintain the smaller 18
395 mooring PIRATA array in the Atlantic. The actual number of sea days required per year
396 to maintain the array may be higher than the absolute minimum though since research
397 cruises sponsored by partner countries often address national scientific priorities in
398 addition to those of the RAMA mission.

399 The greatest impediment to implementation, assuming adequate financial
400 resources and ship time can be found, is vandalism by fishing vessels. Surface buoys are
401 effectively Fish Aggregation Devices (FADs) that attract fish and, consequently,
402 fishermen. Vandalism occurs primarily in pursuit of tuna and affects TAO/TRITON and
403 PIRATA as well as RAMA. Strategies to mitigate vandalism include engineering design
404 improvements to the moorings and outreach to the fishing community. Data losses can
405 also be minimized by scheduling cruises to repair or replace moorings at yearly or more
406 frequent intervals.

407 5. Data and Research Applications

408 RAMA, even in the initial stages of development, is providing valuable data for
409 describing and understanding variability in the Indian Ocean. For example, a pronounced
410 semi-annual cycle in upper ocean temperature, salinity and zonal velocity is evident in
411 the first 3-years of data from near equatorial moorings at 90°E (Fig. 6). Hase et al (2008)
412 relate this variability to remote zonal wind forcing in the central Indian Ocean associated
413 with the monsoon transitions. Upward phase propagation at semi-annual periods in both

414 temperature and zonal velocity is presumably the signature of wind forced equatorial
415 Kelvin waves. This vertical propagation is consistent with, but more sharply defined than,
416 that evident in equatorial time series collected during INDEX in the 1970s (McPhaden,
417 1982; Luyten and Roemmich, 1982). The subsurface salinity maximum centered near
418 100-150 m at 90°E (Fig. 6b) is due to eastward transport along the equator of high
419 salinity water originating in the southern hemisphere subtropics and the Arabian Sea
420 (Taft and Knauss, 1967; Schott et al, 2004). Semi-annual increases in maximum salinity
421 values in this subsurface layer are most likely the response to increases in eastward
422 velocity associated with the semi-annual Wyrtki Jets.

423 Superimposed on these semi-annual variations are energetic 30-50 day period
424 oscillations, which presumably reflect the effects of wind (e.g., Fig. 7a), heat flux, and
425 fresh water forcing on intraseasonal scales. Intraseasonal oscillations are largest for
426 temperature in the thermocline (Fig. 6a) and largest for salinity and zonal velocity in the
427 surface mixed layer (Figs. 6b and 7b). Meridional velocity is most strongly influenced on
428 intraseasonal time scales by 10-20 day period oscillations (Fig. 7c) which are evident not
429 only in the upper 400 m but also at depths greater than 2000 m from the deep ocean
430 moorings along the equator. Sengupta et al. (2004) identified these oscillations as wind
431 forced mixed Rossby-gravity waves.

432 Interannual variability associated with the 2006 IOD event was captured by the
433 moored array as illustrated in the time series from 0°, 80.5°E for two contrasting periods:
434 October-November 2004 and October-November 2006 (Fig. 8). Compared to late 2004,
435 which was near normal in terms of IOD activity (Fig. 2e), zonal surface winds and the
436 zonal mixed layer currents they forced along the equator largely flowed in the opposite

437 direction, i.e. to the west, in late 2006 (Fig. 8a, b). The westward currents drained the
438 eastern basin of upper ocean mass, which may have contributed to periods of thermocline
439 shoaling at 0°, 80.5°E (Fig. 8c). Also, though SST was only slightly warmer than usual at
440 0°, 80.5°E (≤ 1°C) as would be expected for a mooring located outside the IOD SST
441 index regions, these elevated temperatures favored enhanced convection and rainfall in
442 the central basin (Fig. 2). The dramatic drop in mixed layer salinity of over 1 psu in late
443 2006 relative to late 2004 at 0°, 80.5°E (Fig. 8d) is consistent with this enhanced rainfall,
444 as well as with equatorward flow of low salinity water from the Andaman Sea (Murty et
445 al, 2008). It is also interesting to note that the meridional component of mixed layer
446 velocity in Fig. 8b exhibits very regular biweekly oscillations as observed in the 0°, 90°E
447 ADCP data (Fig. 7c) and in the deep ocean moorings along the equator (Sengupta et al,
448 2004).

449 Data from the mooring at 8°S, 67°E in the region of the Seychelles-Chagos
450 thermocline ridge illustrate ocean-atmosphere interactions associated with the passage of
451 tropical cyclone Dora (Duvel et al, 2008; Vialard et al, 2008a). Dora began as a tropical
452 disturbance northeast of the buoy in the vicinity of Diego Garcia (7°S, 72°E) in late
453 January 2007. As this disturbance migrated in south-southwesterly direction, it intensified
454 to named tropical storm strength on January 30 and to tropical cyclone strength on
455 February 1. Dora reached peak intensity of over 100 kts (51 m s^{-1}) on February 3 when it
456 was centered near 18°S, 67°E. Afterwards, it continued to track to the southwest,
457 eventually dissipating by February 12.

458 Dora passed near the buoy in the early stages of its development (January 25-29)
459 before it became a named tropical storm. Its effects in the real-time daily averaged data

460 can be seen in the sudden change in wind speed and direction, increase in precipitation,
461 decrease in atmospheric pressure, and decrease in incoming shortwave radiation at the
462 buoy site in late January 2007 (Fig. 9, left panel). Also evident in late January are abrupt
463 cooling and freshening of the surface mixed layer associated with decreased surface heat
464 fluxes and increased fresh water fluxes. Internally recorded 1- to 10-minute data
465 recovered from the buoy show even greater detail during the last week of January 2007
466 (Fig. 9, right panel). One sees for example a very sharp drop in surface salinity and
467 temperature associated with a nighttime rain event on January 24. Also, SST dropped in a
468 very stepwise fashion by 2°C over the week. Periods of very low insolation on rainy (and
469 presumably cloudy) days are evident. There is also a pronounced solar semi-diurnal tide
470 in atmospheric surface pressure. These data are being analyzed to quantitatively address
471 the relative roles of surface fluxes, vertical turbulent mixing, and horizontal advection in
472 the heat and salt balances for this particular period.

473 RAMA mooring data can also be used to identify deficiencies in currently
474 available surface flux products as a stimulus to their possible improvement. For example,
475 surface heat fluxes were calculated from data at three of RAMA mooring sites for
476 comparison with numerical weather prediction (NWP) model flux products, the
477 International Satellite Cloud Climatology Project (ISCCP) radiation product (Zhang et al,
478 2004) and an objectively analyzed (OA) turbulent heat flux product (OA-Flux; Yu and
479 Weller, 2007). Results (Fig. 10) indicate that that ISCCP overestimates solar radiation
480 and underestimates longwave radiation at these sites. The NWP products significantly
481 overestimate latent heat fluxes such that the net heat flux into the ocean is underestimated
482 by 40-60 W m^{-2} at 0°, 80.5°E. This heat flux deficit, if accumulated in a 50 m thick mixed

483 layer over three months, would translate into a temperature error of ~2°C, which is
484 equivalent to the seasonal range of SST at this location. The OA-Flux product slightly
485 underestimates latent heat fluxes at all three locations, but is a significant improvement
486 on the NWP turbulent fluxes.

487 6. Summary and Discussion

488 RAMA addresses a long-standing need for a sustained moored buoy array in the
489 Indian Ocean for climate studies. It will take several more years to complete and will
490 require coordinated resource contributions (financial, human, and ship time) from several
491 countries. Implementation of RAMA will result in a globe-girdling network of tropical
492 moored buoy arrays that includes TAO/TRITON in the Pacific and PIRATA in the
493 Atlantic. Like these other arrays, we can expect that RAMA will fundamentally advance
494 our understanding of large-scale ocean dynamics, ocean-atmosphere interactions, and
495 climate variability in the Indian Ocean region.

496 We can also expect that RAMA will contribute to operational activities as a
497 component of GOOS, the Global Climate Observing System (GCOS), and the Global
498 Earth Observing System of Systems (GEOSS). Real-time RAMA data available on the
499 GTS are, for example, already being incorporated into weather forecasts and seasonal
500 climate forecasts produced by operational centers. RAMA can likewise provide valuable
501 data for operational ocean state estimation and for oceanic and atmospheric reanalysis
502 products. The array will provide data for validating satellite retrievals and products based
503 on them such as for surface winds, SST, rainfall, and mixed layer currents. Finally,
504 RAMA data will be valuable for quantitatively assessing the performance of oceanic and
505 atmospheric dynamical models.

RAMA moorings, and in particular those specially instrumented reference sites for air-sea heat, moisture and momentum fluxes, are a contribution to the Ocean Sustained Interdisciplinary Timeseries Environment observation System (OceanSITES), a worldwide network of deep water stations providing high temporal resolution data for ocean research and environmental forecasting (http://www.oceansites.org/). In addition, RAMA is capable of accommodating biogeochemical sensors to support programs such as the International Ocean Carbon Coordination Project (IOCCP; http://www.ioccp.org/) and the Sustained Indian Ocean Biogeochemical and Ecological Research (SIBER) program (Hood et al, 2008). RAMA will provide information on oceanic variability for the Joint Aerosol-Monsoon Experiment (JAMEX; Lau et al, 2008), which is a multi-national study scheduled for 2007-11 to investigate the effects of aerosols on ocean-atmosphere-land interactions that govern the Asian monsoon water cycle. In the wake of the December 2004 Asian tsunami, discussions are also underway with organizations involved in developing the Indian Ocean tsunami warning system on how best to coordinate implementation efforts with IndOOS. A joint RAMA and tsunami mooring cruise has already been conducted aboard the Indonesian Research Vessel Baruna Jaya III in September 2007 (http://www.noaanews.noaa.gov/stories2007/s2919.htm). In the longer term, it may beneficial to consider development of a multi-hazard moored buoy platform for both tsunami warnings and climate studies.

RAMA mooring stations provide convenient focal points around with to conduct short term process studies such as MISMO, which took place in October-December 2006 centered at 0°, 80.5°E, and VASCO-Cirene which took place in January-February 2007 near the mooring at 8°S, 67°E in the Seychelles-Chagos thermocline ridge region. These

process studies benefited from RAMA because they examined ocean-atmosphere interactions associated with the MJO for which high resolution moored time series data are especially valuable (e.g. Vialard et al, 2008b). RAMA in turn can benefit from process studies, since new knowledge gained from programs like MISMO and VASCO-Cirene can feedback into design specifications for the moored array. Moreover, the VASCO-Cirene field campaign provided an opportunity to deploy the flux reference site mooring at 8°S, 67°E.

Neither RAMA nor IndOOS will address all the observational needs for understanding and predicting climate variability in the region since we still lack a sustained, in situ observing system for the atmosphere over the Indian Ocean. This lack of atmospheric data limits our understanding of convective processes, atmospheric circulation, and interactions of the atmosphere with the ocean. Regular cruises to service RAMA moorings can help mitigate this problem though by providing platforms of opportunity for routine meteorological observations.

In summary, full implementation of RAMA promises significant scientific and societal benefits. Challenges that we must overcome include securing the necessary resources to complete the array and forging long-lasting multi-national partnerships to sustain it. We know that success is possible though because it has been achieved in the past for similar mooring programs of ambitious scope in the tropical Pacific and Atlantic.

548 Acknowledgments

549 The authors would like to thank an anonymous reviewer, H. Annamalai, and the
550 BAMS subject matter editor Brian Mapes for helpful comments on an earlier version of
551 this manuscript. We also acknowledge the International CLIVAR Project Office and the
552 Intergovernmental Oceanographic Commission Perth Regional Office for supporting the
553 Indian Ocean Panel. Many institutions and organizations have contributed to the
554 implementation of RAMA and deserve mention: in India, the Ministry of Earth Sciences,
555 the Indian National Center for Ocean Information Services and the National Institute of
556 Oceanography; in Japan, the Japan Agency for Marine-Earth Science and Technology
557 and the Ministry of Education, Sports, Culture, Science and Technology; in China, the
558 State Oceanic Administration, First Institute of Oceanography, and Ministry of Science
559 and Technology; in Indonesia, the Agency for the Assessment and Application of
560 Technology and the Agency for Marine and Fisheries Research; in France the Institut
561 Français de Recherche pour l'Exploitation de la Mer, the Institut de Recherche pour le
562 Développement and the Institut National des Sciences de l'Univers; in South Africa, the
563 University of Capetown and the Agulhas and Somali Current Large Marine Ecosystems
564 Project implemented by the United Nations Development Programme through funding
565 from the Global Environment Facility; in the U.S., the NOAA Climate Program Office
566 and the Office of Climate Observation. This manuscript was initiated while the first
567 author was a guest at the University of Tasmania's Integrated Marine Observing System
568 Office in Hobart, Australia. PMEL publication number 3199 and NIO contribution
569 number 4437. We dedicate this paper to the memory of our friend and colleague Fritz
570 Schott, who inspired us through his scientific leadership, wise counsel, and deep

571 understanding of the ocean.

572 References

573 Alory, G., S. Wijffels, and G. Meyers,2007: Observed temperature trends in the Indian
574 Ocean over 1960—1999 and associated mechanisms, Geophys. Res. Lett., 34, L02606,
575 doi:10.1029/2006GL028044.

576 Annamalai H., and R. Murtugudde, 2004: Role of the Indian Ocean in regional climate
577 variability. Earth's Climate: The Ocean-Atmosphere Interaction, Geophys. Monogr., No.
578 147, Amer. Geophys. Union, 213–246.
579
580 Annamalai, H., H. Okajima, and M. Watanabe, 2007: Possible Impact of the Indian
581 Ocean SST on the Northern Hemisphere Circulation during El Niño. J. Climate, 20,
582 3164–3189.
583
584 Arguez, A., 2007: Supplement to State of the Climate in 2006. Bull. Amer. Meteor. Soc.,
585 88, s1–s135.
586
587 Ashok K., W.-L. Chan, T. Motoi, T. Yamagata, 2004: Decadal variability of the Indian
588 Ocean dipole, Geophys. Res. Lett., 31, L24207, doi:10.1029/2004GL021345.
589
590 Bessafi, M. and M.C. Wheeler, 2006: Modulation of south Indian ocean tropical cyclones
591 by the Madden-Julian oscillation and convectively coupled equatorial waves, Mon. Wea.
592 Rev., 134, 638-656.
593
594 Bhat, G. S., S. Gadgil, P.V. Hareesh Kumar, S. R. Kalsi, P. Madhusoodanan, V. S. N.
595 Murty, C. V. K. Prasada Rao, V. Ramesh Babu, L. V. G. Rao, R. R. Rao, M.
596 Ravichandran, K. G. Reddy, P. Sanjeeva Rao, D. Sengupta, D. R. Sikka, J. Swain, and P.
597 N. Vinayachandran, 2001: BOBMEX: The Bay of Bengal Monsoon Experiment. *Bull.*
598 *Am. Meteorol. Soc.*, 82, 2217-2243.
599
600 Bonjean, F. and Lagerloef, G. E. S.: Diagnostic Model and Analysis of the Surface
601 Currents in the Tropical Pacific Ocean, 2002: J. Phys. Oceanogr., 32, 2938–2954, 2002.
602
603 Bourlès, B., R. Lumpkin, M. J. McPhaden, F. Hernandez, P. Nobre, E. Campos, L. Yu, S.
604 Planton, A. J. Busalacchi, A. D. Moura, J. Servain, and J. Trotte, 2008: The PIRATA
605 Program: History, Accomplishments, and Future Directions. *Bull. Amer. Meteorol. Soc.,*
606 89, 1111-1125.
607
608 Chang, P., T. Yamagata, P. Schopf, S.K. Behera, J. Carton, W.S. Kessler, G. Meyers, T.
609 Qu, F. Schott, S. Shetye, and S.P. Xie, 2006: Climate Fluctuations of Tropical Coupled
610 Systems—The Role of Ocean Dynamics. J. Climate, 19, 5122–5174.
611
612 Cherchi, A., S. Gualdi, S. Behera, J. J. Luo, S. Masson, T. Yamagata, and A. Navarra,
613 2007: The Influence of Tropical Indian Ocean SST on the Indian Summer Monsoon. J.
614 Climate, 20, 3083–3105.
615

Clark, C.O., J. E. Cole, and P. J. Webster, 2000: Indian Ocean SST and Indian Summer Rainfall: Predictive Relationships and Their Decadal Variability. J. Climate, 13, 2503–2519.

CLIVAR-GOOS Indian Ocean Panel, 2006: Understanding the role of the Indian Ocean in the climate system - Implementation Plan for sustained observations. ICPO Publication Series #100, International CLIVAR Project Office, Southampton, UK, 76pp.

Cutler, A.N., Swallow, J.C., 1984. Surface currents of the Indian ocean (to 25°S, 100°E): Compiled from historical data archived by the meteorological office, Bracknell, U.K., IOS Report No. 187, 8pp, 36 charts.

de Ruijter, W. P. M., A. Biastoch, S. S. Drijfhout, J. R. E. Lutjeharms, R. P. Matano, T. Pichevin, P. J. van Leeuwen, and W. Weijer, 1999: Indian-Atlantic interocean exchange: Dynamics, estimation and impact, J. Geophys. Res., 104(C9), 20,885–20,910.

Duvel, J.P., and J. Vialard, 2007: Indo-Pacific Sea Surface Temperature Perturbations Associated with Intraseasonal Oscillations of Tropical Convection. J. Climate, 20, 3056–3082.

Duvel, J-P., C. Basdevant, H. Bellenger, G. Reverdin, A. Vargas and J. Vialard, 2008: The Aeroclipper: A new device to explore convective systems and cyclones, *Bull. Am. Met. Soc*, in press.

ECMWF, 1994: The description of the ECMWF/WCRP level III-A atmospheric data archive. Technical Attachment, ECMWF Shinfield Park, Reading, UK, 72pp.

Fairall, C. F., E. F. Bradley, J. E. Hare, A. A. Grachev, and J. B. Edson, 2003: Bulk parameterization of air-sea fluxes: Updates and verification for the COARE algorithm, *J. Climate*, 16, 571–591.

Feng, M., G. Meyers, and S. Wijffels, 2001: Interannual Upper Ocean Variability in the Tropical Indian Ocean, Geophys. Res. Lett., 28(21), 4151–4154.

Fu, L.L., 2007: Intraseasonal Variability of the Equatorial Indian Ocean Observed from Sea Surface Height, Wind, and Temperature Data. J. Phys. Oceanogr., 37, 188–202.

Giannini, A., R. Saravanan, and P. Chang, 2003: Oceanic forcing of Sahel rainfall on interannual to interdecadal time scales, Science, 302, 1027–1030.

Gordon, A. L., 2001: Interocean exchange. In: Ocean Circulation and Climate, G. Siedler, J. Church and J. Gould (eds.), Academic Press, pp. 303-314.

Gordon, Arnold L., 2005: Oceanography of the Indonesian Seas and their Throughflow. Oceanography 18, 14-27.

662 Han, W., P. Webster, R. Lukas, P. Hacker, and A. Hu, 2004: Impact of Atmospheric
663 Intraseasonal Variability in the Indian Ocean: Low-Frequency Rectification in Equatorial
664 Surface Current and Transport. J. Phys. Oceanogr., 34, 1350–1372.
665
666 Han, W., 2005: Origins and Dynamics of the 90-Day and 30–60-Day Variations in the
667 Equatorial Indian Ocean. J. Phys. Oceanogr., 35, 708–728.
668
669 Harrison, D. E., and M. Carson, 2007: Is the World Ocean Warming? Upper-Ocean
670 Temperature Trends: 1950–2000. J. Phys. Oceanogr., 37, 174–187.
671
672 Hase, H., Y. Masumoto, Y. Kuroda, and K. Mizuno, 2008: Semiannual variability in
673 temperature and salinity observed by Triangle Trans-Ocean Buoy Network (TRITON)
674 buoys in the eastern tropical Indian Ocean, J. Geophys. Res., 113, C01016,
675 doi:10.1029/2006JC004026.
676
677 Hermes, J. C. and C. J. C. Reason, 2008: Annual cycle of the South Indian Ocean
678 (Seychelles-Chagos) thermocline ridge in a regional ocean model. J. Geophys. Res.,
679 doi:10.1029/2007JC004363, in press.
680
681 Higgins, R.W., and K.C. Mo, 1997: Persistent North Pacific Circulation Anomalies and
682 the Tropical Intraseasonal Oscillation. J. Climate, 10, 223–244.
683
684 Hoerling, M. P., J. W. Hurrell, and T. Xu, 2001: Tropical Origins for Recent North
685 Atlantic Climate Change. Science, 292, 90-92.
686
687 Hoerling, M., and A. Kumar, 2003: The perfect ocean for drought, Science, 299, 691–
688 694.
689
690 Hood, R. R., A. Naqvi, J. D. Wiggert, J. Goes, V.Coles, J. McCreary, N. Bates, P. K.
691 Karuppasamy, N. Mahowald, S. Seitzinger, and G. Meyers, 2008: Research opportunities
692 and challanges in the Indian Ocean. Eos Trans. AGU, 89(13), 125-26.
693
694 Izumo, T., C. de Boyer Montegut, J-J. Luo, S.K. Behera, S. Masson and T. Yamagata,
695 2008: The role of the western Arabian Sea upwelling in Indian monsoon rainfall
696 variability, J. Climate, accepted.
697
698 Janowiak, J. E. and Xie, P., 1999: CAMS OPI: A Global Satellite-Rain Gauge Merged
699 Product for Real-Time Precipitation Monitoring Applications, J. Climate, 12, 3335–3342.
700
701 Josey, S. A., E. C. Kent, and P. K. Taylor, 1999: New insights into the ocean heat budget
702 closure problem from analysis of the SOC air–sea flux climatology. J. Climate, 12, 2850–
703 2880.
704
705 Kalnay, E., and Coauthors, 1996: The NCEP/NCAR 40-Year Reanalysis Project. Bull.
706 Amer. Meteor. Soc., **77,** 437–471.
707

Kanamitsu, M., W. Ebisuzaki, J. Woolen, J. Potter, S-K Yang, J.J. Hnilo, M. Fiorino, and G. L. Potter, 2002: NCEP-DEO AMIP-II Reanalysis (R-2). Bull. Atmos. Met. Soc., **83,** 1631–1643.

Knauss, J. A., 1961: The International Indian Ocean Expedition. Science, 134, 1674-1676.

Knox, R. A., 1976: On a long series of measurements of Indian Ocean equatorial currents near Addu Atoll. Deep-Sea Res., 23, 211-222.

Kuroda Y. and Y. Amitani, 2000: TRITON--New ocean and atmospheric observing buoy network for monitoring ENSO, Umi no Kenkyu, 10, 157-172.

Krishnamurti, T., 1985: Summer Monsoon Experiment—A Review. Mon. Wea. Rev., 113, 1590–1626.

Lau, K.-M. and Co-authors, 2008: The joint aerosol-monsoon experiment: A new challenge for monsoon climate research. Bull. Am. Meteorol. Soc., 89. 369-381.

Lee, T. and M.J. McPhaden, 2008: Decadal phase change in large-scale sea level and winds in the Indo-Pacific region at the end of the 20th century. Geophys. Res. Lett., 35, L01605, doi:10.1029/2007GL032419.

Lee, T. and M.J. McPhaden, 2008: Decadal phase change in large-scale sea level and winds in the Indo-Pacific region at the end of the 20th century. Geophys. Res. Lett., 35, L01605, doi:10.1029/2007GL032419.

Levitus, S., J. Antonov, and T. Boyer, 2005: Warming of the world ocean, 1955 – 2003, Geophys. Res. Lett., 32, L02604, doi:10.1029/ 2004GL021592.

Liebmann, B., H. H. Hendon and J. D. Glick, 1994: The Relationship between tropical cyclone of the Western Pacific and Indian Oceans and the Madden-Julian Oscillation, J. Met. Soc. Jap., 72, 401-412.

Luo, J. J., S. Masson, S. Behera, and T. Yamagata, 2007: Experimental Forecasts of the Indian Ocean Dipole Using a Coupled OAGCM. J. Climate, 20, 2178–2190.

Luyten, J. R., M. Fieux, and J. Gonella, 1980: Equatorial currents in the western Indian Ocean. Science, 209, 600-603.

Luyten, J.R., and D.H. Roemmich, 1982: Equatorial Currents at Semi-Annual Period in the Indian Ocean. J. Phys. Oceanogr., 12, 406–413.

Madden, R.A., and P.R. Julian, 1994: Observations of the 40–50-Day Tropical Oscillation—A Review. Mon. Wea. Rev., 122, 814–837.

Maloney, E.D., and D.L. Hartmann, 2000: Modulation of hurricane activity in the Gulf of Mexico by the Madden–Julian Oscillation. Science, 287, 2002-2004.

Masumoto, Y., H. Hase, Y. Kuroda, H. Matsuura, and K. Takeuchi, 2005: Intraseasonal variability in the upper layer currents observed in the eastern equatorial Indian Ocean. *Geophys. Res. Lett.,* **32**, L02607, doi:10.1029/2004GL021896.

McPhaden, M. J., 1999: Genesis and evolution of the 1997–98 El Niño, Science, 283, 950–954.

McPhaden, M. J., A. J. Busalacchi, R. Cheney, J. R. Donguy, K. S. Gage, D. Halpern, M. Ji, P. Julian, G. Meyers, G. T. Mitchum, P. P. Niiler, J. Picaut, R. W. Reynolds, N. Smith, K. Takeuchi, 1998: The Tropical Ocean-Global Atmosphere (TOGA) observing system: A decade of progress. J. Geophys. Res., 103, 14,169-14,240.

McPhaden M. J., Y. Kuroda, and V. S. N. Murty, 2006: Development of an Indian Ocean Moored Buoy Array for Climate Studies. CLIVAR Exchanges, 11(4), International CLIVAR Project Office, Southampton, UK, p. 3-5.

McPhaden, M.J., X. Zhang, H.H. Hendon, and M.C. Wheeler, 2006: Large Scale Dynamics and MJO Forcing of ENSO Variability. Geophys. Res. Lett., 33(16), L16702, doi:10.1029/2006GL026786.

Meyers, G. and R. Boscolo, 2006: The Indian Ocean Observing System (IndOOS). CLIVAR Exchanges, 11(4), International CLIVAR Project Office, Southampton, UK, p. 2-3.

Meyers, G., P. McIntosh, L. Pigot, and M. Pook, 2007: The Years of El Niño, La Niña, and Interactions with the Tropical Indian Ocean. J. Climate, 20, 2872–2880.

Meyers, Gary and Roger Proctor, 2008: The Australian Integrated Marine Observing System. J. Ocean Technol., in press.

Miura, H., M. Satoh, T. Nasuno, A. T. Noda, and K. Oouchi, 2007: A Madden-Julian Oscillation Event Realistically Simulated by a Global Cloud-Resolving Model, 318, 1763-1765.

Murty, V. S. N., M.S.S. Sarma, A. Suryanarayana, D. Sengupta, A. S. Unnikrishnan,V. Fernando, A. Almeida, S. Khalap, A. Sardar, K. Somasundar, and M. Ravichandran, 2006: Indian Moorings: Deep-sea current meter moorings in the Eastern Equatorial Indian Ocean. CLIVAR Exchanges, 11(4), International CLIVAR Project Office, Southampton, UK, p. 5-8.

Murty, V.S.N., Bulusu Subrahmanyam, S. Muralikrishna, David M. Heffner, A.S.N. Lakshmi, C. Neelima and P. J. Vidya, 2008: Seasonal and Interannual Variability of Sea Surface Salinity during 2002-06 from Argo profiles and OGCM simulations in the tropical Indian Ocean. J. Geophys. Res., in revision.

National Research Council, 1996: Learning to predict climate variations associated with El Niño and the southern oscillation. Accomplishments and legacies of the TOGA Program. National Academy Press, Washington, D.C., 171 pp.
National Research Council, 2000: Fifty Years of Discovery: National Science Foundation 1950-2000. National Academy Press, Washington, DC, 270 pp.

Oke, P. R., and A. Schiller, 2007: A Model-Based Assessment and Design of a Tropical Indian Ocean Mooring Array. J. Climate, 20, 3269–3283.

Reppin, J., F. Schott, J. Fishcher, and D. Quadfasel, 1999: Equatorial currents and transports in the upper central Indian Ocean. *J. Geophys. Res*., **104**, 15495-15514.

Reynolds, R. W., Rayner, N. A., Smith, T. M., Stokes, D. C., and Wang, W. Q., 2002: An improved in situ and satellite SST analysis for climate, J. Climate, 15, 1609–1625.

Ridderinkhof, H. and W. P. M. De Ruijter, 2003: Moored current observations in the Mozambique Channel. Deep-Sea Res. II, 50: 1933-1955.

Rudnick, D. L., R. A. Weller, C. C. Eriksen, T. D. Dickey, J. Marra, and C. Langdon, 1997: Moored instruments weather Arabian Sea monsoons, yield data. EOS, *Trans. Am. Geophys. Union* **78**, 117, 120-121.

Saji, N. H., B. N. Goswami, P. N. Vinayachandran and T. Yamagata, 1999: A dipole mode in the tropical Indian Ocean. *Nature,* **401,** 360-363.

Sanjeeva Rao, P. and D. R. Sikka, 2005: Intraseasonal Variability of the summer monsoon over the North Indian Ocean as revealed by the BOBMEX and ARMEX field Programs, Pure Appl. Geophys. 162, 1481–1510.

Schott, F., and J. P. McCreary, 2001: The monsoon circulation of the Indian Ocean, Prog. Oceanogr., 51, 1-123.

Schott, F. A., J. P. McCreary, and G. C. Johnson, 2004: Shallow over-turning circulations of the tropical-subtropical oceans. In Earth Climate: The Ocean-Atmosphere Interaction. C. Wang, S.-P. Xie, and J. Carton (eds.), *Geophys. Monograph,* **147**, AGU, Washington, D.C., p. 261-304.

Schott, F. A., S.-P. Xie, and J. P. McCreary, 2008: Indian Ocean circulation and climate variability. Rev. Geophys., in press.

Seiki, A., and Y.N. Takayabu, 2007: Westerly Wind Bursts and Their Relationship with Intraseasonal Variations and ENSO. Part I: Statistics. Mon. Wea. Rev., 135, 3325–3345.

Sengupta, D., R. Senan, B.N. Goswami and J. Vialard, 2007: Intraseasonal variability of equatorial Indian Ocean zonal currents, *Journal of Climate,* **20,** 3036-3055.

Sengupta, D., R. Senan, V. S. N. Murty, and V. Fernando, 2004: A biweekly mode in the equatorial Indian Ocean. *J. Geophys. Res.,* **109,** C10003, doi:10.1029/2004JC002329.

Shenoi, S. S. C., D. Shankar, and S. R. Shetye, 2002: Differences in heat budgets of the near surface Arabian Sea and Bay of Bengal: Implications for the summer monsoon, *Journal of Geophysical Research*, *107*, C6, 10.1029/2000JC000679.

Shinoda, T., and W. Han, 2005: Influence of the Indian Ocean Dipole on Atmospheric Subseasonal Variability. J. Climate, 18, 3891–3909.

Siedler, G., J. Church and J. Gould (eds.), 2001: Ocean Circulation and Climate - Observing and Modelling the Global Ocean. Academic Press, San Diego, 715pp.

Slingo, J. M., et al., 1996: Intraseasonal oscillations in 15 atmospheric general circulation models: Results from an AMIP diagnostic subproject, Clim. Dyn., 12, 325–357.

Smith, S. L., 2001: Understanding the Arabian Sea: Reflections on the 1994–1996 Arabian Sea Expedition. Deep-Sea Res. Part II: Topical Studies in Oceanography, 48, 1385-1402.

Syamsudin, F., A. Kaneko, and D. B. Haidvogel, 2004: Numerical and observational estimates of Indian Ocean Kelvin wave intrusion into Lombok Strait. Geophys. Res. Lett., L24307, doi:10.1029/2004GL021227.

Taft, B. A. and J. A. Knauss, 1967: The equatorial undercurrent in the Indian Ocean as observed by the Lusiad Expedition. Bull. Scripps Inst. Oceanogr., 9, 163pp.

Uppala, S., and Coauthors, 2005: The ERA-40 re-analysis. Quart. J. Roy. Meteor. Soc., **131,** 2961–3012.

Vecchi, G.A. and D.E. Harrison, 2004: Interannual Indian rainfall variability and Indian Ocean sea surface temperature anomalies. In *Earth Climate: The Ocean-Atmosphere Interaction,* C. Wang, S.-P. Xie, and J.A. Carton (eds.), American Geophysical Union, Geophysical Monograph 147, Washington D.C., 247-260.

Vecchi, G.A., and M.J. Harrison, 2007: An Observing System Simulation Experiment for the Indian Ocean. J. Climate, 20, 3300–3319.

Vialard, J., J.P. Duvel, M. McPhaden, P. Bouruet-Aubertot, B. Ward, E. Key, D. Bourras, R. Weller, P. Minnett, A. Weill, C. Cassou, L. Eymard, T. Fristedt, C. Basdevant, Y. Dandoneau, O. Duteil, T. Izumo, C. de Boyer Montégut, S. Masson1, F. Marsac, 2008a: Cirene: Air-sea interactions in the Seychelles-Chagos thermocline ridge region. Bull. Am. Meteorol. Soc., in press.

Vialard, J., G. Foltz, M. McPhaden, J.P. Duvel, and C. de Boyer Montégut, 2008b: Strong Indian Ocean cooling driven by the Madden-Julian oscillation in late 2007 and early 2008. Geophys. Res. Lett., in press.

Wainwright, L., G. Meyers, S.Wijffels, and L. Pigot, 2008: Change in the Indonesian Throughflow with the climate shift of 1966/77. Geophys. Res. Lett., L03604, doi:10.1029/2007GL031911.

Waliser D. E., K.-M. Lau, and J.-H. Kim, 1999: The Influence of Coupled Sea Surface Temperatures on the Madden-Julian Oscillation: A ModelPerturbation Experiment. J. Atmos. Sci., 56, 333-358.

Wajsowicz, R. C., 2005: Potential predictability of tropical Indian Ocean SST anomalies, Geophys. Res. Lett., 32, L24702, doi:10.1029/2005GL024169.

Waple, A. M., and J. H. Lawrimore, 2003: State of the Climate in 2002. Bull. Amer. Meteor. Soc., 84, 800.

Webster, P. W., A. M. Moore, J. P. Loschnigg and R. R. Lebben, 1999: Coupled ocean-atmosphere dynamics in the Indian Ocean during 1997-98, *Nature*, **401**, 356-360.

Webster, P. J., E. F. Bradley, C. W. Fairall, J. S. Godfray, P. Hacker, R. A. Houze Jr., R. Lukas, Y. Serra, J. M. Hummon, T. D. M. Lawrence, C. A. Russell, M. N. Ryan, K. Sahami, and P. Zuidema, 2002: The JASMINE pilot study. Bull. Am. Meteorol. Soc., 83, 1603-1630.

Webster, P. J, and C. Hoyos, 2004: Prediction of Monsoon Rainfall and River Discharge on 15-30 day Time Scales. Bull. Am. Meteorol. Soc., 85, 1745-1765.

Wijffels, S. and G. Meyers, 2004: An intersection of oceanic waveguides—variability in the Indonesian throughflow region. *J. Phys. Oceanogr.* **34**, 1232-1253.

Woolnough S. J., F. Vitart, and M. Balmaseda, 2007: The role of the ocean in the Madden-Julian Oscillation: Sensitivity of an MJO forecast to ocean coupling. Quart. J. Roy. Meteor. Soc., 133, 117–128.

Xie, S.P., H. Annamalai, F. A. Schott, and J. P. McCreary, 2002: Structure and Mechanisms of South Indian Ocean Climate Variability. J. Climate, 15, 864–878.

Yang, J., Q. Liu, S.-P. Xie, Z. Liu, and L. Wu, 2007: Impact of the Indian Ocean SST basin mode on the Asian summer monsoon, Geophys. Res. Lett., 34, L02708, doi:10.1029/2006GL028571.

Yaremchuk, M., 2006: Sea surface salinity constrains rainfall estimates over tropical oceans, Geophys. Res. Lett., 33, L15605, doi:10.1029/2006GL026582.

Yokoi, T., T. Tozuka and T. Yamagata, 2008: Seasonal variation of the Seychelles

938 Dome. J. Clim.,21, 3740-3754.
939
940 Yoneyama, K. et al, 2008: MISMO field experiment in the tropical Indian Ocean. Bull.
941 Am. Meteor. Soc., in press.
942
943 Yu, W., B. Xiang, L. Liu, and N. Liu, 2005: Understanding the origins of interannual
944 thermocline variations in the tropical Indian Ocean. Geophys. Res. Lett., 32, L24706,
945 doi:10.1029/2005GL024327.
946
947 Yu, L., X. Jin, and R.A. Weller, 2007: Annual, Seasonal, and Interannual Variability of
948 Air–Sea Heat Fluxes in the Indian Ocean. J. Climate, 20, 3190–3209.
949
950 Yu, L., and R.A. Weller, 2007: Objectively Analyzed Air–Sea Heat Fluxes for the Global
951 Ice-Free Oceans (1981–2005). Bull. Amer. Meteor. Soc., 88, 527–539.
952
953 Yu, Z., and J. P. McCreary Jr., 2004; Assessing precipitation products in the Indian
954 Ocean using an ocean model, J. Geophys. Res., 109, C05013,
955 doi:10.1029/2003JC002106.
956
957 Zhang, C., 2005: Madden-Julian Oscillation, Rev. Geophys., 43, RG2003,
958 doi:10.1029/2004RG000158.
959
960 Zhang, Y., W. B. Rossow, A. A. Lacis, V. Oinas, and M. I. Mishchenko, 2004:
961 Calculation of radiative fluxes from the surface to top of atmosphere based on ISCCP and
962 other global data sets: Refinements of the radiative transfer model and the input data, J.
963 Geophys. Res., 109, D19105, doi:10.1029/2003JD004457.
964

SIDE BOX 1. RAMA Helps Australian Farmers

"No summer rain, then enough to sow in April/May on the arable country, but the plains still missed out. This meant feeding sheep all through autumn and a very low lambing percentage. Then…." Susan Carn is recounting the interplay between weather patterns and management of her farm the past season. She and her husband Ben raise sheep in the low rainfall area of the Flinders Ranges in South Australia. "So looking back … I'm really glad I stuck to my guns and told my husband to stop sowing as things were not adding up for a good season."

Susan is also the science liaison for the BestPrac farming group in the region. She knows a lot about climate and is always on the look-out for new streams of information to support the decisions they must make throughout the year. The Indian Ocean Dipole affects rainfall in their region and Susan was using RAMA data provided by the Indian Ocean Panel as an indicator of evolving Dipole conditions. The Panel was happy to hear this report: "Thank you for sending me the TRITON info. Back in July I showed it to my BestPrac group who all thought it scary but very useful!"

Modern farmers have many sources of information available to them for improving their bottom lines. Climate information is just one of the sources, but farmers and climate researchers are forging new links to exploit that information. The BestPrac Group meets regularly to share experiences that can enhance their farm management skills. An important part of each meeting is to review the latest seasonal forecasts from the Australian Bureau of Meteorology along with climate indices such as the Southern Oscillation Index and the Indian Ocean Dipole Index. Data from sources like RAMA moorings are also factored into the deliberations. This information helps the farmers to

make informed decisions on a range of practices such as cropping programs, fertilizer and spray applications, and stocking rates (i.e., the number of animals to keep on the property). The group can then better cope with climate related risks and capitalize on opportunities. Their motto is "Hope is not a plan!"

A BestPrac meeting with members immersed in study. Susan and Ben are on the left. Photo credit: John Squires.

BestPrac members fat-scoring sheep to determine if they need supplementary feeding. Photo credit: John Squires.

SIDE BOX 2: RAMA moorings

Four types of moorings are presently used in RAMA: surface moorings, surface moorings with enhanced measurement capabilities for comprehensive air-sea fluxes (i.e., "flux reference site" moorings), ADCP moorings, and deep-ocean moorings. Each mooring type is described briefly below.

The surface moorings consist of both Autonomous Temperature Line Acquisition System (ATLAS) moorings and two different types of Triangle Trans Ocean Buoy Network (TRITON) moorings. These moorings have a design lifetime of one year and so must be serviced annually. Most of the surface moorings are ATLAS moorings supplied by NOAA's Pacific Marine Environmental Laboratory (PMEL). These taut line surface moorings are anchored to the ocean floor in depths of typically 2500-5000 m. Measurements on the surface float include air temperature, relative humidity, wind velocity, downwelling shortwave radiation, and rain rate at heights of 3-4 m above mean sea level. Sea surface temperature and conductivity (which together yield salinity) are measured from the buoy at a nominal depth of 1 m. Sensors on the mooring line measure ocean temperature (12 depths between 10 m and 500 m), conductivity (5 depths between 10 m and 100 m), mixed layer velocity (at 10 m depth) and pressure (at two depths). A detailed description of the individual sensors, including their heights and depths relative to mean sea level, is contained in the electronic supplement. Daily averages of all data and several hourly samples per day of most meteorological variables are transmitted to shore in real-time via Service Argos. These data are placed on the Global Telecommunications System (GTS) for use in operational weather, climate, and ocean forecasting. Higher temporal resolution data (at 1- to 10-minute intervals in most cases)

1024 are internally recorded and available after mooring recovery.

1025 Some ATLAS moorings are enhanced with additional instrumentation to more
1026 precisely define surface heat, moisture and momentum fluxes. These flux reference site
1027 moorings include sensors for downwelling longwave radiation and barometric pressure.
1028 Additional sensors may also be deployed in the upper 140 m of the ocean for finer
1029 vertical resolution measurements of temperature, salinity and velocity. Additional
1030 information on ATLAS moorings can be found at
1031 http://www.pmel.noaa.gov/tao/proj_over/mooring.shtml .

1032 The Japan Marine-Earth Science and Technology Agency (JAMSTEC) has
1033 deployed TRITON moorings and, since February 2008, mini-TRITON (m-TRITON)
1034 moorings at 1.5°S, 90°E and 5°S, 95°E. TRITON moorings are taut-line moorings
1035 designed to be functionally equivalent to ATLAS moorings in terms of sensor payloads,
1036 temporal resolution, and data accuracy. There are some differences (e.g. TRITON
1037 moorings are deployed with more salinity sensors and measurements are made to 750 m
1038 rather than 500 m), but these differences do not affect comparability of the basic data
1039 sets.

1040 After one-year inter-comparison with the TRITON mooring at 1.5°S, 90°E,
1041 JAMSTEC began to deploy m-TRITON moorings at 1.5°S, 90°E and 5°S, 95°E in
1042 February 2008. The m-TRITON sensor and signal processing system are based on those
1043 for TRITON, but the mooring system itself is slack line rather than taut-line. Slack line
1044 moorings allow for substantial vertical excursions of subsurface sensors due to variable
1045 currents and winds. Thus, all m-TRITON subsurface sensors are equipped to measure
1046 pressure so that the shape of the mooring line can be determined, after which temperature

and salinity data can be interpolated to standard depths.

Hourly averages of all TRITON and m-TRITON data are transmitted to shore in real-time via Service Argos and placed on the GTS. Higher temporal resolution data (at 1- to 10-minute intervals in most cases) are internally recorded and available after mooring recovery. TRITON and m-TRITON sensor specifications, including heights and depths relative to mean sea level, are described in the electronic supplement. More information on TRITON and m-TRITON moorings can be found at http://www.jamstec.go.jp/jamstec/TRITON/real_time/overview.php/po.php and http://www.jamstec.go.jp/iorgc/iomics/index.html, respectively.

Acoustic Doppler Current Profiler (ADCP) moorings are deployed at several locations in the array. The ADCP is positioned with its acoustic beams pointing upward in a subsurface float typically located at depths 300-400 m below the surface. Velocity profiles are measured at hourly intervals with 8 m vertical resolution. Backscatter from the ocean surface interferes with velocity retrievals in the upper 30-40 m of the water column, so subsurface ADCPs do not measure effectively in this depth range. Hence the need for current meters in the mixed layer on surface moorings. ADCP data are available upon mooring recovery. More information on ADCP specifications can be found in the electronic supplement.

Deep ocean moorings maintained by India's National Institute of Oceanography (NIO) have a subsurface float nominally at 100 m depth, below which 6 mechanical current meters are attached to the mooring line for velocity measurements down to a depth of approximately 4000 m. Beginning in 2003, upward-pointing ADCPs similar to those used by PMEL and JAMSTEC were added to the near surface float for additional

velocity measurements. Data at 1-2 hourly intervals are available from these moorings on recovery. More technical information on these moorings can be found in the electronic supplement and in Murty et al (2006).

A web portal with pointers to data from all moorings is found at http://www.incois.gov.in/Incois/iogoos/home_indoos.jsp. Subsets of the data are available from http://www.pmel.noaa.gov/tao/, http://www.jamstec.go.jp/jamstec/TRITON/real_time/php/top.php, and http://www.nio.org/data_info/deep-sea_mooring/oos-deep-sea-currentmeter-moorings.htm.

SIDE BOX 3: RAMA Implementation Time Line

RAMA traces its roots to Indian and Japanese national efforts initiated in 2000. JAMSTEC deployed an ADCP mooring at 0°, 90°E in 2000 (Masumoto et al, 2005) and two TRITON moorings at 1.5°S, 90°E and 5°S, 95°E in 2001 (Hase et al, 2008). NIO also began subsurface mooring deployments to sample the deep ocean along the equator in 2000 (Sengupta et al, 2004; Murty et al, 2006). These efforts, which have continued without interruption, were precursors to RAMA and incorporated into the array design.

Then, in October-November 2004, NOAA/PMEL in collaboration with NIO and the Indian Ministry of Earth Sciences (MoES) deployed four ATLAS moorings and one ADCP mooring near the equator between 80°-90°E. PMEL and the Indonesian Agency for the Assessment and Application of Technology (BPPT) and the Ministry for Marine Affairs and Fisheries (DKP) occupied sites at 4°N, 90°E and 8°N, 89°E in November 2006. The French-lead VASCO-Cirene experiment (Duvel et al, 2008; Vialard et al, 2008a) provided an opportunity in January 2007 to establish the flux reference site ATLAS mooring at 8°S, 67°E. In November 2007, a Chinese ADCP mooring was deployed off the coast of Java as part of a collaboration between the Chinese First Institute of Oceanography (FIO), BPPT, and DKP. Also in November 2007, PMEL and Indian technicians deployed two ATLAS moorings in the Bay of Bengal (12°N and 15°N, 90°E) on a cruise lead by the Indian National Center for Ocean Information Services (INCOIS). In November 2008, the Agulhas and Somali Current Large Marine Ecosystems (ASCLME) Project, a consortium of eight African countries, joined the RAMA fold by deploying two ATLAS moorings along 55°E (8°S and 12°S) from the

Norwegian RV Dr Fridtjof Nansen. The ASCLME includes Kenya, Tanzania, Mozambique, South Africa, Madagascar, Mauritius, Seychelles, and Comoros.

Efforts to build and sustain the array will continue within a framework of formal bilateral agreements that are either approved or under development between agencies in the various partner countries. Our expectation based on current and projected resource commitments is that RAMA will be completed by the end of 2012. The precise implementation time line cannot be determined in detail at this time though since not all formal agreements are finalized yet.

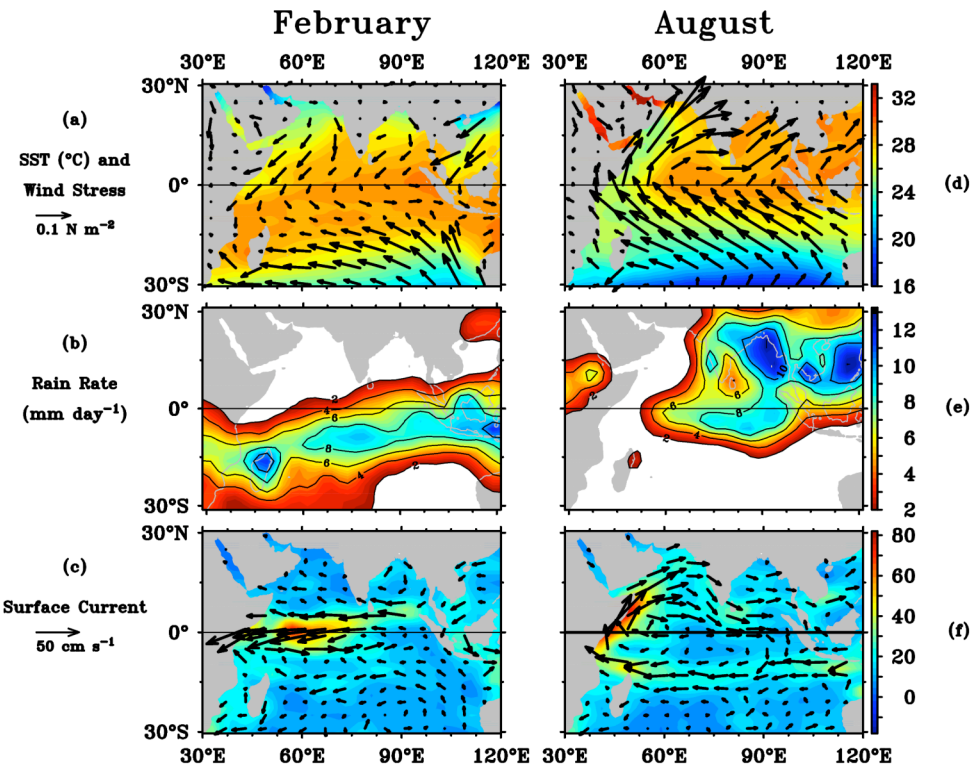

Figure 1. Monthly means for February of (a) surface wind stress and SST; (b) rain rate; and (c) surface current velocity (vectors) and scalar speed (color shading). Corresponding monthly means for August are in (d)-(f). Rain rate is contoured only for values ≥ 2 mm day^{-1}. SSTs are based on Reynolds et al. (2002), winds are from the ECMWF-ERA40 reanalysis dataset (http://data.ecmwf.int/data/d/era40_daily/), currents are from Cutler and Swallow (1984), and rain rate is from an analysis of satellite and in situ raingauge data (Janowiak and Xie, 1999).

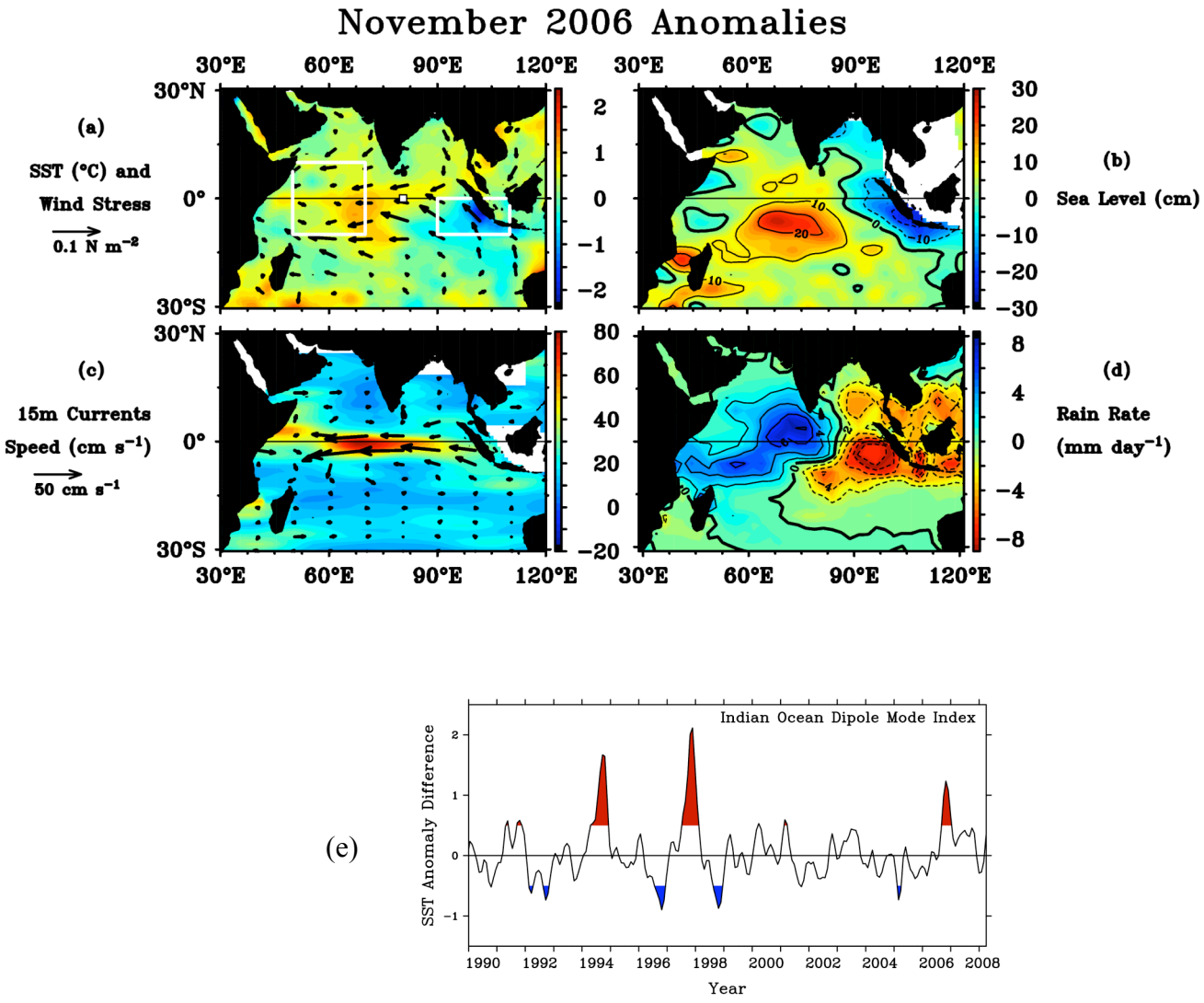

Figure 2. Monthly anomalies from the mean seasonal cycle in November 2006 for (a) SST (based on Reynolds et al., 2002) and QuikSCAT wind stress (http://www.ifremer.fr/cersat/); (b) Jason satellite altimeter sea level anomalies; (c) current velocity (vectors) and speeds (color shading) representative of flow at 15 m depth in the surface mixed layer (Bonjean and Lagerloef, 2002); (d) rain rate (Janowiak and Xie, 1999). Shown in (e) is the IOD index for 1990-2008, with the strongest positive events (index > 0.5°C) and negative events (index is < -0.5°C) highlighted in red and blue respectively. The index represents the difference between SST anomalies in the western minus the eastern basin regions outlined in (a). Also shown in (a) is the location of an ATLAS mooring at 0°, 80.5°E, time series of which are shown in Figure 8.

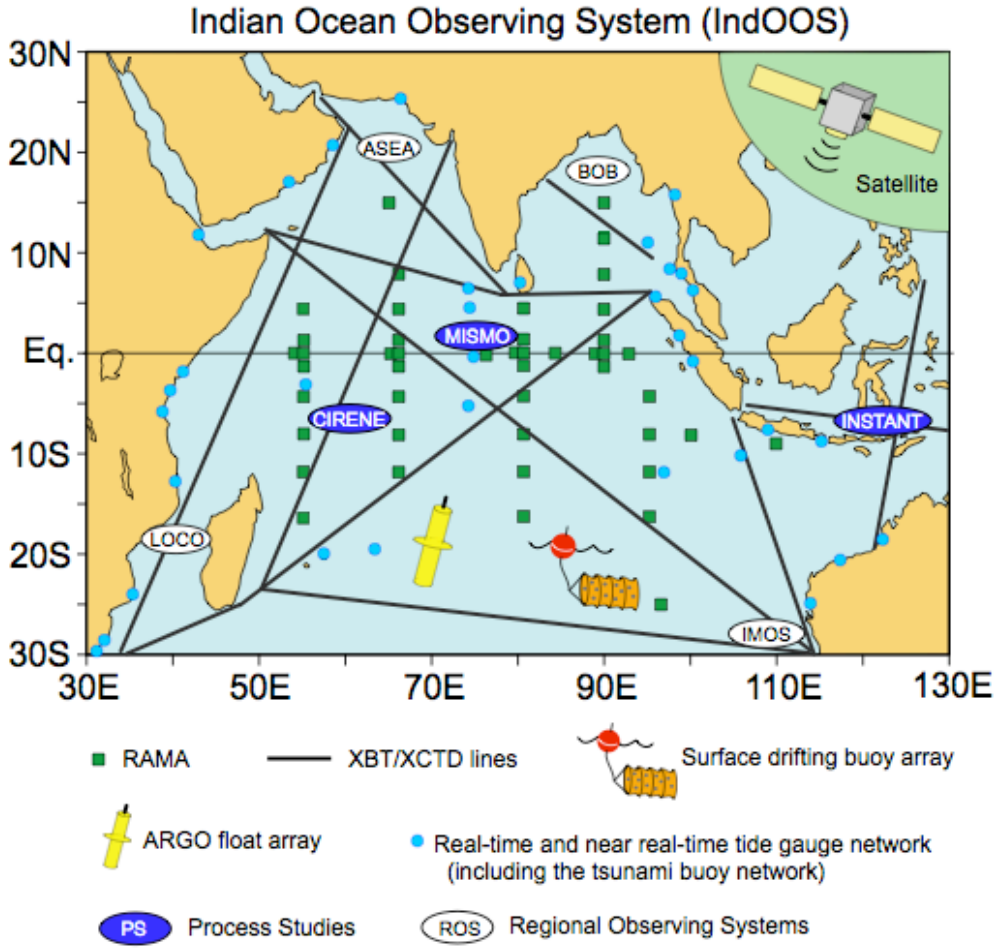

Figure 3. Schematic of the Indian Ocean Observing System (IndOOS). Green squares indicate the locations of RAMA moorings. Tide gauges are indicated by blue dots. Argo floats and surface drifters are indicated by a single symbol although many of each are spread throughout the basin (141 drifters and 296 Argo floats as of 31 August 2008). Expendable bathythermograph (XBT) and expendable conductivity/temperature/depth (XCTD) sections sampled by ships-of-opportunity are shown as black lines. Most of these lines are sampled 12-18 times per year at along-track intervals of approximately 1° (though the Australia-Sumatra line and the Australia-Mauritius-South Africa are sampled more frequently to measure details of ocean circulation). Nationally sponsored regional observing systems (ROS) are shown in ovals: IMOS, LOCO, Arabian Sea (ASEA), and Bay of Bengal (BOB). Process studies (PS) are shown in blue ovals: MISMO, VASCO-Cirene and INSTANT. The satellite in the upper right symbolizes the constellation of Earth-observing satellites for SST, surface winds, sea level, and other important oceanic and atmospheric parameters.

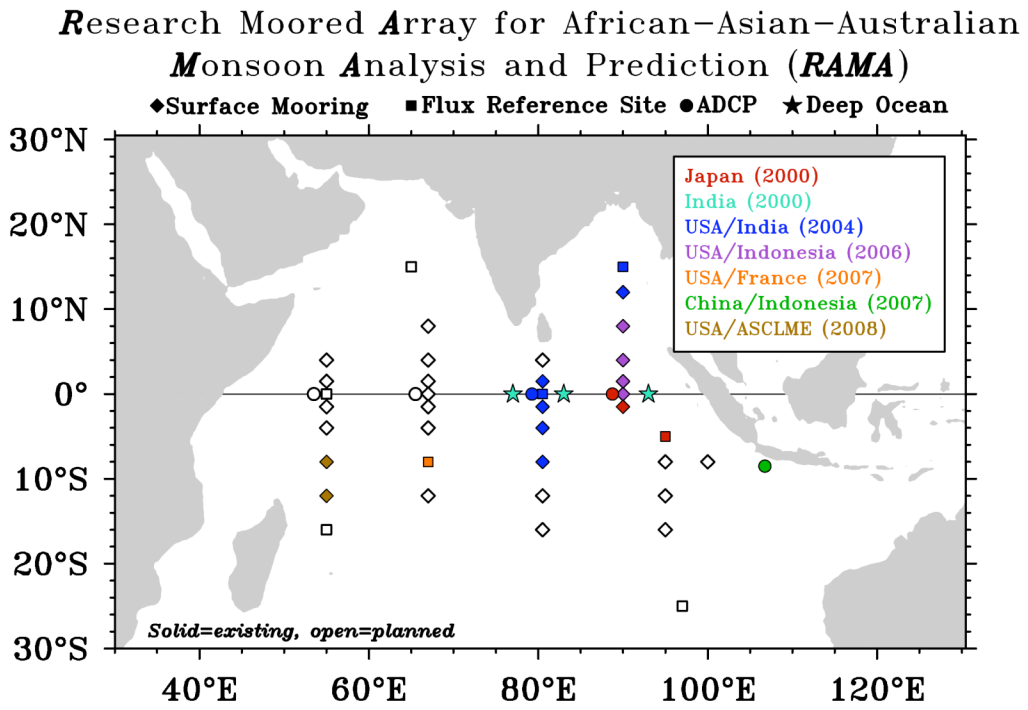

Figure 4. Schematic of RAMA as of December 2008. Solid symbols indicate those sites occupied so far. Color coding indicates national support, with year of first involvement shown in the upper right box. Open symbols indicate sites that are not yet instrumented. ASCLME is a consortium of eight African nations including Kenya, Tanzania, Mozambique, South Africa, Madagascar, Mauritius, Seychelles, and Comoros.

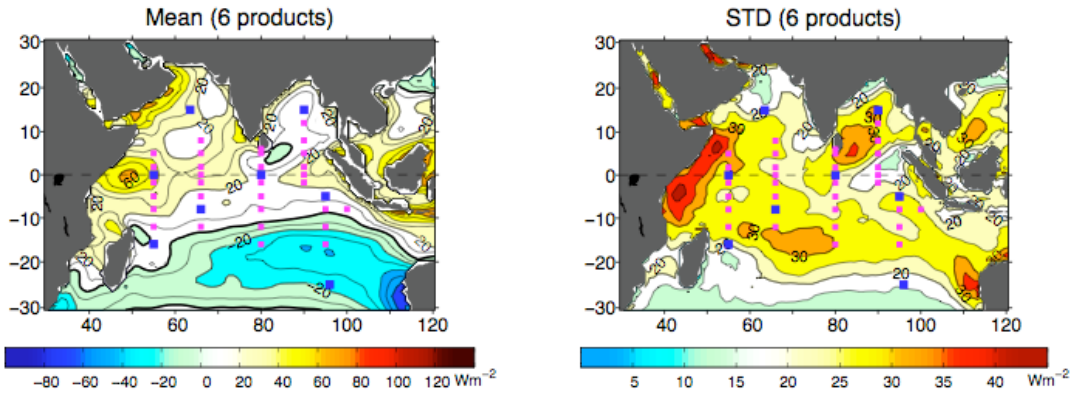

(a) (b)

Figure 5. The (a) average and (b) standard deviation of long term mean net heat fluxes from six different products. The RAMA array is superimposed on these fields with flux reference sites highlighted as blue squares. The six products are: the National Centers for Environmental Prediction NCEP1 (Kalnay et al, 1996) and NCEP2 (Kanamitsu et al, 2002) fluxes; European Center for Medium Range Forecasting (ECMWF) operational fluxes (ECMWF, 1994); ECMWF reanalysis fluxes (ERA40; Uppala et al, 2005); the U.K. National Oceanography Center (NOC) fluxes (Josey et al, 1999); and an objectively analyzed turbulent surface heat flux product produced by Woods Hole Oceanographic Institution (OA-Flux; Yu and Weller, 2007) combined with radiation data from the International Satellite Cloud Climatology Project (ISSCP; Zhang et al, 2004). Long term means for NCEP1, NCEP2, OAFlux+ISCCP, and ECMWF are based on the period 1983-2004; ERA40 means were based on the period 1983-2001 and the NOC climatology was based the period on 1980-2005.

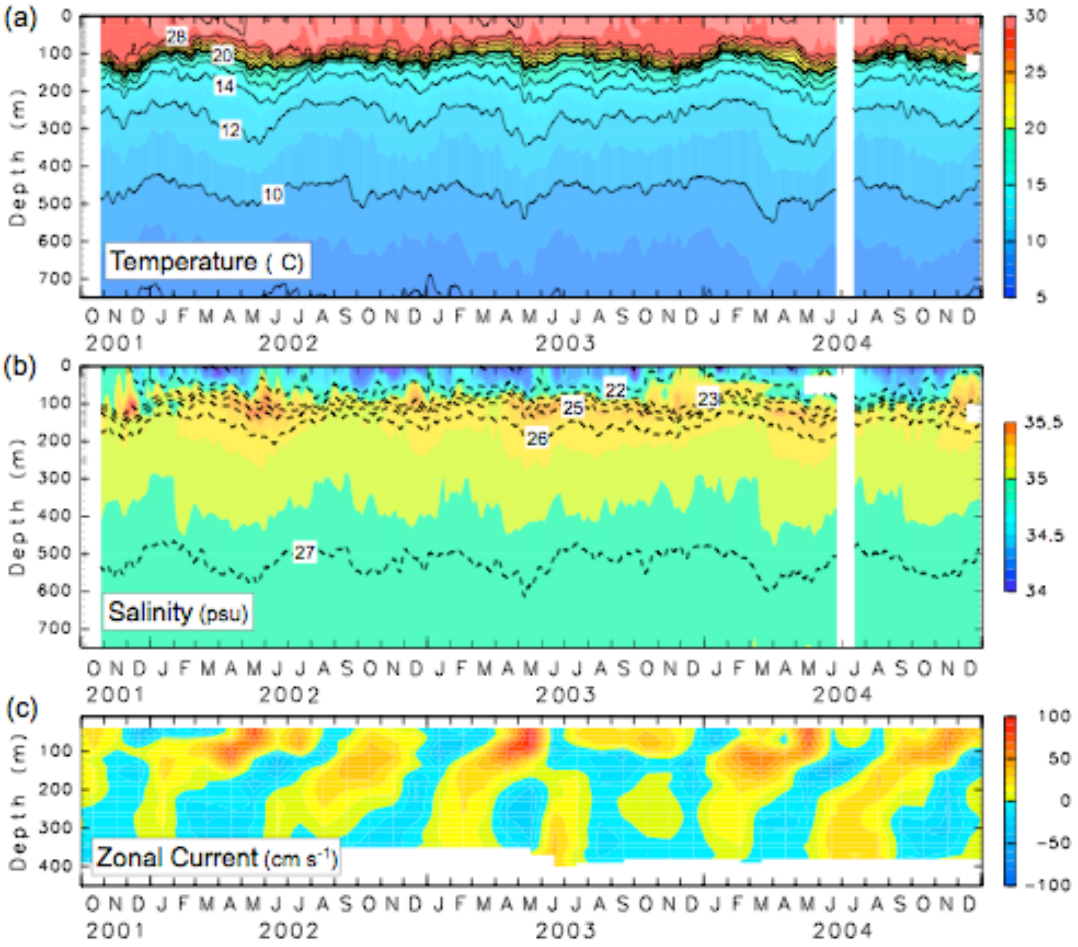

Figure 6. Time/depth sections of (a) temperature and (b) salinity from 1.5°S, 90°E and (c) zonal velocity from 0°, 90°E. Daily data in (a) and (b) have been smoothed with a 7-day running mean filter and in (c) with a monthly filter. Color intervals for the temperature, salinity and velocity are 1°C, 0.1, and 10 cm s^{-1}, respectively. Thin black lines are at intervals of 2°C for temperature with 20°C isotherm shown as a thick line. Contours of the potential density at intervals of 1.0 kg m^{-3} are superimposed on salinity sections (after Hase et al, 2008).

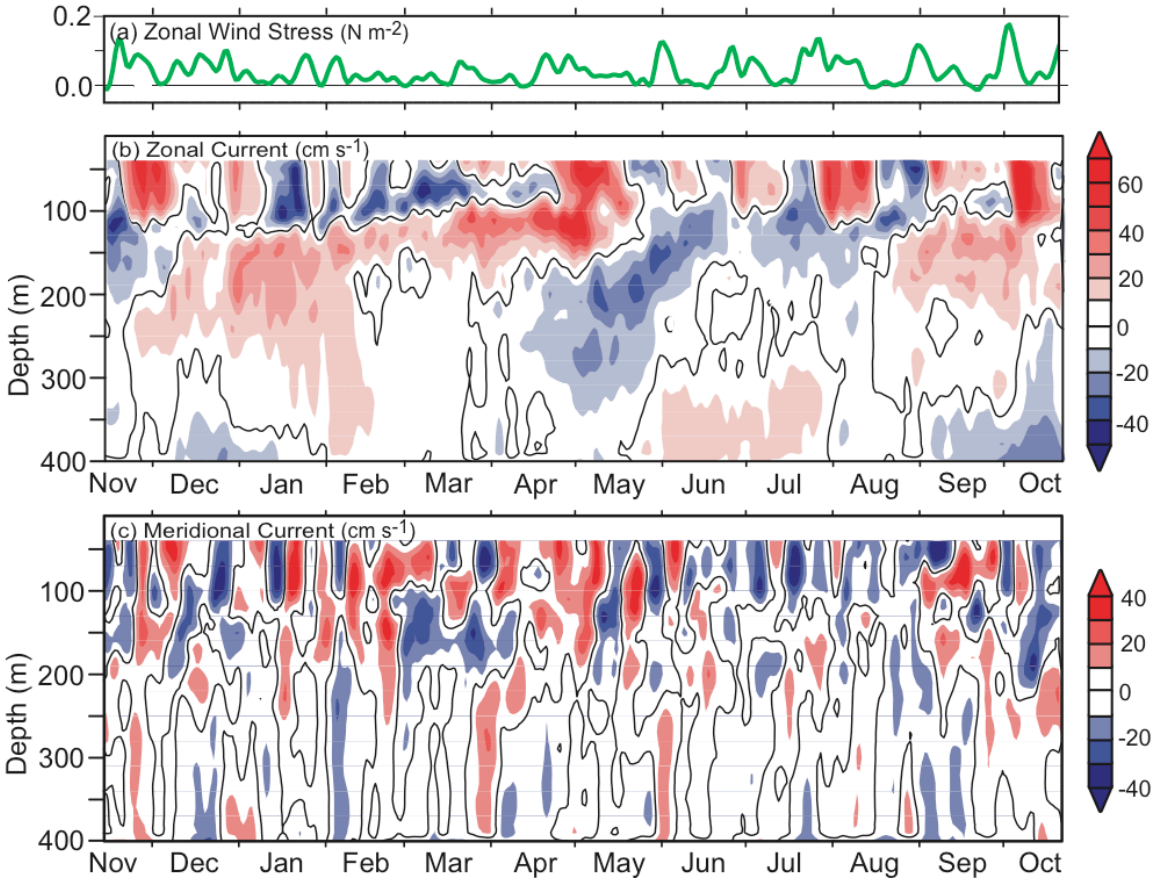

Figure 7. Time series of (a) zonal wind stress (in N m^{-2}) at the sea surface averaged between 80°E and 90°E observed by the QuickSCAT satellite. Time-depth sections of (b) zonal current and (c) the meridional current observed at 0°, 90°E. The eastward (westward) and northward (southward) currents are shaded in reds (blues), with black contours for zero velocity. Daily data have been low pass filtered with a 5-day period cut off (after Masumoto et al, 2005).

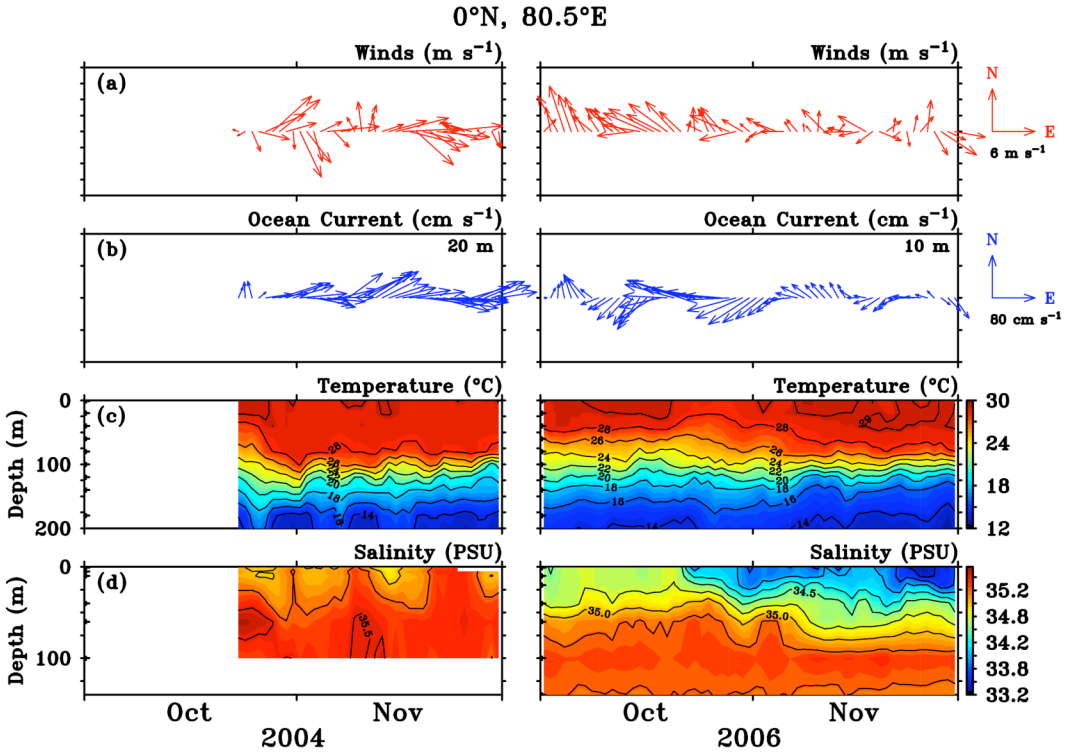

Figure 8. Daily averaged data at 0°, 80.5°E for October-November 2004 (a neutral IOD year) and October-November 2006 (a positive IOD year, as illustrated in Fig. 2). Shown are (a) wind vectors, (b) velocity vectors in the mixed layer (20 m depth in 2004 and 10 m depth in 2006), (c) temperature and (d) salinity. Start of the time series in mid-October 2004 is coincident with the first deployment at this site.

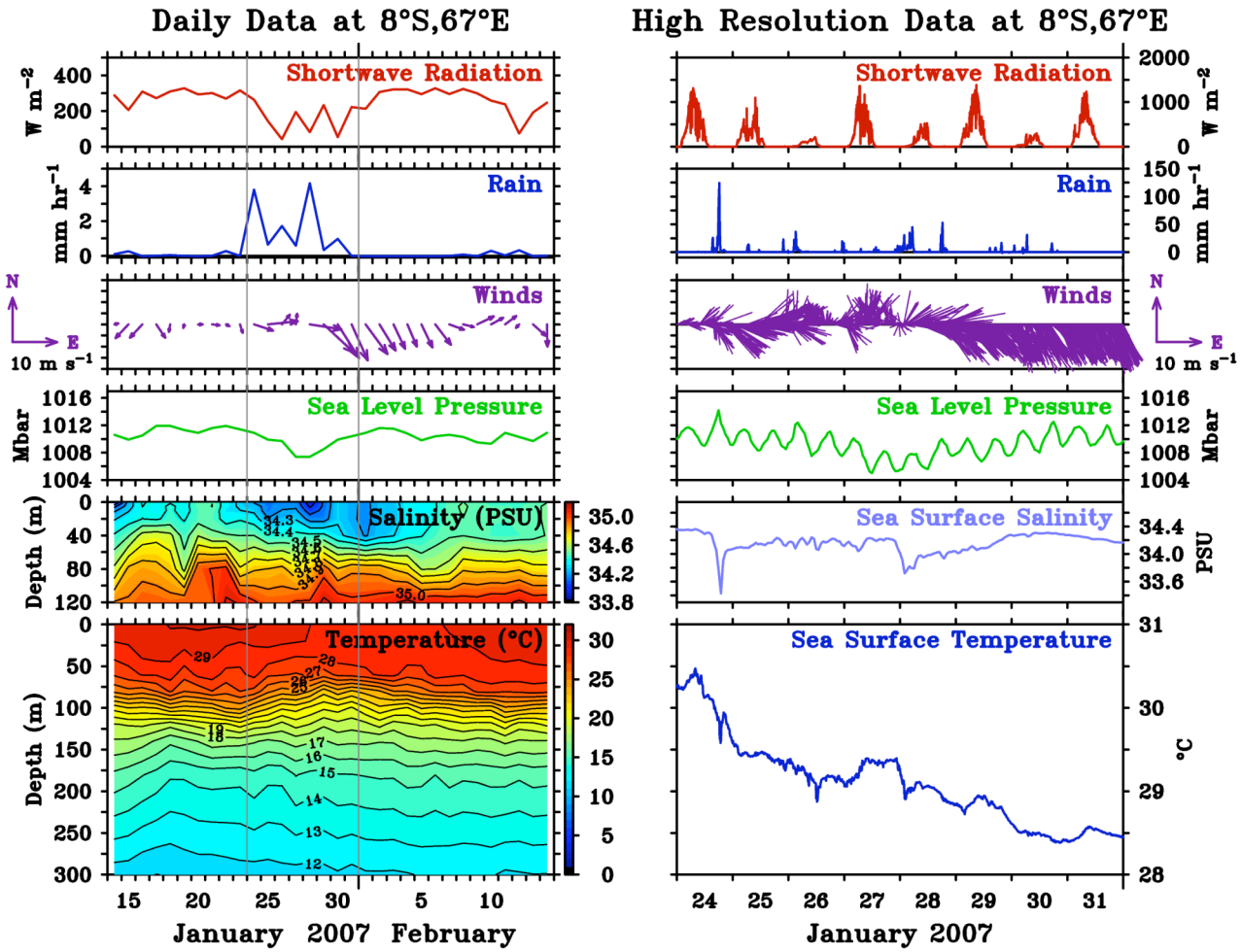

Figure 9. Time series data from 8°S, 67°E in the Seychelles-Chagos thermocline ridge region during January-February 2007. Left panel shows daily averaged real-time data whereas the right panel shows hourly averages based internally recorded data for selected variables during the week of January 24-31. The period highlighted on the right (delineated in the left panel by light grey lines) coincides with the passage nearby of tropical cyclone Dora in the early stages of its development. Arrow heads have been left off the vector winds in left panel for clarity.

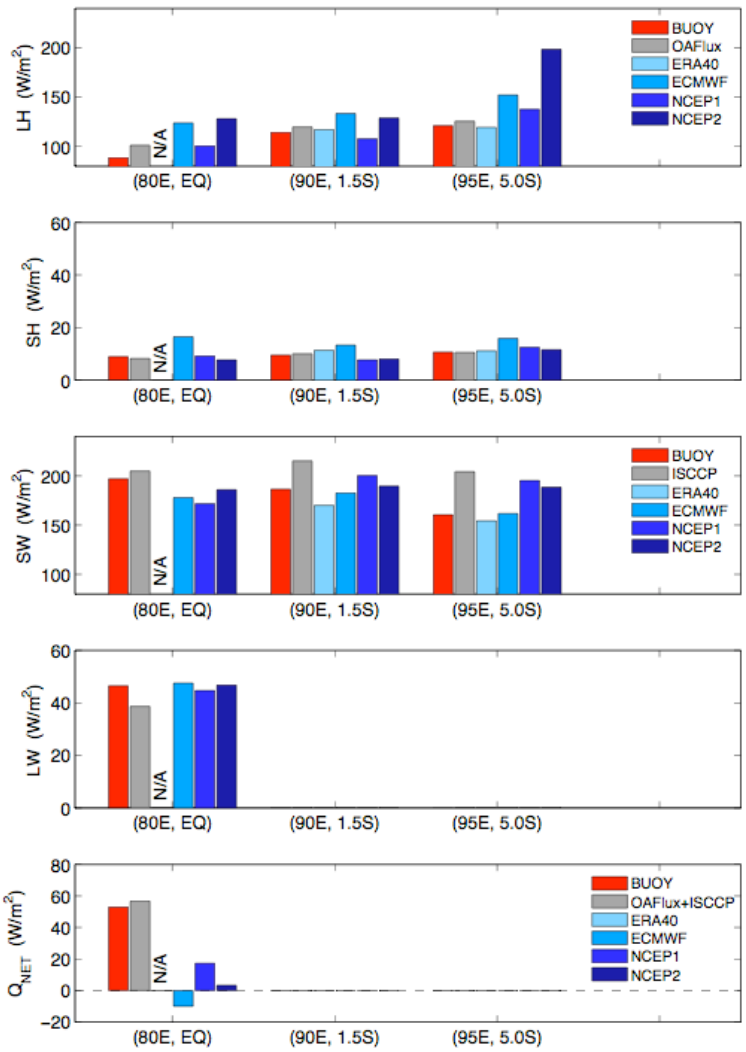

Figure 10. Comparison of surface heat flux components at three RAMA sites with those computed from six different research and operational surface flux products: NCEP1, NCEP2, ECMWF, ERA40, OA-Flux, and ISCCP (see Figure 5 caption for product definitions and references). Fluxes are, from top to bottom, latent heat flux (LH), sensible heat flux (SH), net shortwave radiation (SW), net longwave radiation (LW), and net surface heat flux (Q_{net}). Direct measurements of downwelling longwave radiation were made only at 0°, 80.5°E. Hence, LW and Q_{net} (which represents the sum of the four individual components) are shown only for this site. Turbulent fluxes were computed with the COARE version 3.0 flux algorithm (Fairall et al, 2003) using daily averaged data. No warm layer cool skin corrections were applied. Shortwave radiation was adjusted for 6% albedo. Upwelling longwave radiation at 0°, 80.5°E was computed assuming blackbody radiation from the sea surface with an emissivity of 0.97. Comparisons were based on 70 days of overlapping data at 0°, 80.5°E between 23 Oct 2004 to 31 Dec 2004; 310 days of overlapping data at 1.5°S, 90°E between 23 Oct 2001 and 31 Aug 2002; and 287 days of overlapping data at 5°S, 95°E between 26 Oct 2001 and 31 Aug 2002.